THE JOURNAL OF BIOLOGICAL CHEMISTRY
Vol. 278, No. 48, Issue of November 28, pp. 48367–48376, 2003
Printed in U.S.A.

Cooperative Roles of Fyn and Cortactin in Cell Migration of Metastatic Murine Melanoma*

Received for publication, July 28, 2003, and in revised form, September 12, 2003
Published, JBC Papers in Press, September 16, 2003, DOI 10.1074/jbc.M308213200

Jinhong Huang‡§¶, Tamae Asawa‡, Tsuyoshi Takato‖, and Ryuichi Sakai‡**

From the ‡Growth Factor Division, National Cancer Center Research Institute, 5-1-1 Tsukiji, Chuo-ku, Tokyo 104-0045, Japan, the ‖Department of Oral and Maxillofacial Surgery, University of Tokyo, 7-3-1 Hongo, Bunkyo-ku, Tokyo 113-8655, Japan, and the §Laboratory for Molecular Neurogenesis, RIKEN Brain Science Institute, 2-1 Hirosawa, Wako, Saitama 351-0198, Japan

Src family kinases are major regulators of various integrin-mediated biological processes, although their functional roles and substrates in cancer metastasis are unknown. We explored the roles of Src family tyrosine kinases in cell migration and the spread of K-1735 murine melanoma cell lines with low or high metastatic potential. Corresponding to elevated cell motility and spreading ability, Fyn was selectively activated among Src family kinases, and the cell motility was blocked by an inhibitor of Src family kinases. Significant tyrosine phosphorylation of cortactin, stable complex formation between activated Fyn and cortactin, and co-localization of cortactin with Fyn at cell membranes were all observed only in cells with high metastatic potential. Both integrin-mediated Fyn activation and hyperphosphorylation of cortactin were observed 2–5 h after stimulation in highly metastatic cells, and they required *de novo* protein synthesis. We demonstrate that cortactin is a specific substrate and cooperative effector of Fyn in integrin-mediated signaling processes regulating metastatic potential.

Malignant tumors are thought to contain subpopulations of cells with differential metastatic capabilities (1). Processes of tumor metastasis consist of multiple steps linked together, including invasion, detachment, intravasation, circulation, adhesion, extravasation, and growth in distant organs (2). Cell locomotion and spreading are key functions of the cells required in most of these processes. Analysis of differences in expression and modification of signaling molecules associated with cell migration and spreading among tumor sublines with different metastatic potentials in a tumor is expected to provide precise information for understanding the molecular mechanisms underlying the development of cancer metastasis.

There are studies demonstrating that Src family tyrosine kinases play essential roles in the signaling of integrin-mediated biological processes such as actin organization and cell migration (3–7). In addition, recent reports show that Src is highly activated in colon cancers, particularly in those metastatic to the liver (8). Involvement of Src kinase during metastatic spread of carcinoma cells in NBT-II rat carcinoma cell lines has also been suggested (5). Fyn has been suggested a factor governing the metastatic potential of tumors including murine methylcholanthrene-induced fibrosarcoma cells (9), although the precise mechanism is unknown.

Increasing numbers of studies have shown that Src family kinases function through collaboration with their substrates, such as FAK, cortactin, $p130^{Cas}$ (a Crk-associated substrate), and paxillin in cytoskeleton organization and cell migration. FAK is activated upon cell binding to extracellular matrix proteins and forms transient signaling complexes with Src family kinases (10). Cortactin plays essential roles in cortical actin cytoskeleton organization, primarily affecting cell motility and invasion (11–13). A docking protein, $p130^{Cas}$, plays essential roles in cell attachment and migration when it is tyrosine-phosphorylated by Src family kinases (6). Functional roles of paxillin in integrin-mediated signaling have been implicated by tyrosine phosphorylation of paxillin following integrin-dependent cell adhesion to extracellular matrix proteins, which is in part attributed to Src family kinases (14). To obtain further information on their involvements in the progression of metastasis, appropriate biological models showing different metastatic potentials are required.

A widely used model for studying the molecular mechanisms underlying the progression of metastasis is a series of cell lines derived from K-1735 murine melanoma, which contains heterogeneous clones with multiple metastatic diversities (15). The primary K-1735 melanoma that arose in an inbred C3H/HeN murine mammary tumor virus-negative mouse was transplanted once into an immunosuppressed recipient and then established in culture. Randomly chosen clones C10 and C19 were classified as nonmetastatic or low metastatic; M2 and X21 were highly metastatic and produce tumor foci in lungs of syngenic mice (15). In this study, we investigated the roles of Src family tyrosine kinases in cell migration and the spread of these cell lines. Up-regulation of Fyn kinase activity and enhanced tyrosine phosphorylation of cortactin were identified in highly metastatic cells, which also showed elevated cell motility and spreading ability. A new mode of integrin-mediated activation of Fyn was also observed in highly metastatic cells. These results indicate a novel role of the Fyn-cortactin pathway required for the regulation of cell motility and metastatic potential during the progression of metastasis.

EXPERIMENTAL PROCEDURES

Cells and Cell Culture—K-1735-derived mouse melanoma cell lines were donated by Dr. I. J. Fidler. Clones C-10 and C-19 are classified as nonmetastatic or low metastatic. Parental clones M-2 and X21 are highly metastatic and produce tumor foci in lungs of syngenic mice (15).

* This work was supported by the Program for Promotion of Fundamental Studies in Health Science of Organization for Pharmaceutical Safety and Research of Japan. The costs of publication of this article were defrayed in part by the payment of page charges. This article must therefore be hereby marked "*advertisement*" in accordance with 18 U.S.C. Section 1734 solely to indicate this fact.

¶ Supported by a scholarship from HonJo International Scholarship Foundation.

** To whom correspondence should be addressed: Growth Factor Division, National Cancer Center Research Institute, 5-1-1 Tsukiji, Chuo-ku, Tokyo 104-0045, Japan. Tel: 03-3542-2511 (ext. 4300); Fax: 03-3542-8170; E-mail: rsakai@gan2.res.ncc.go.jp.

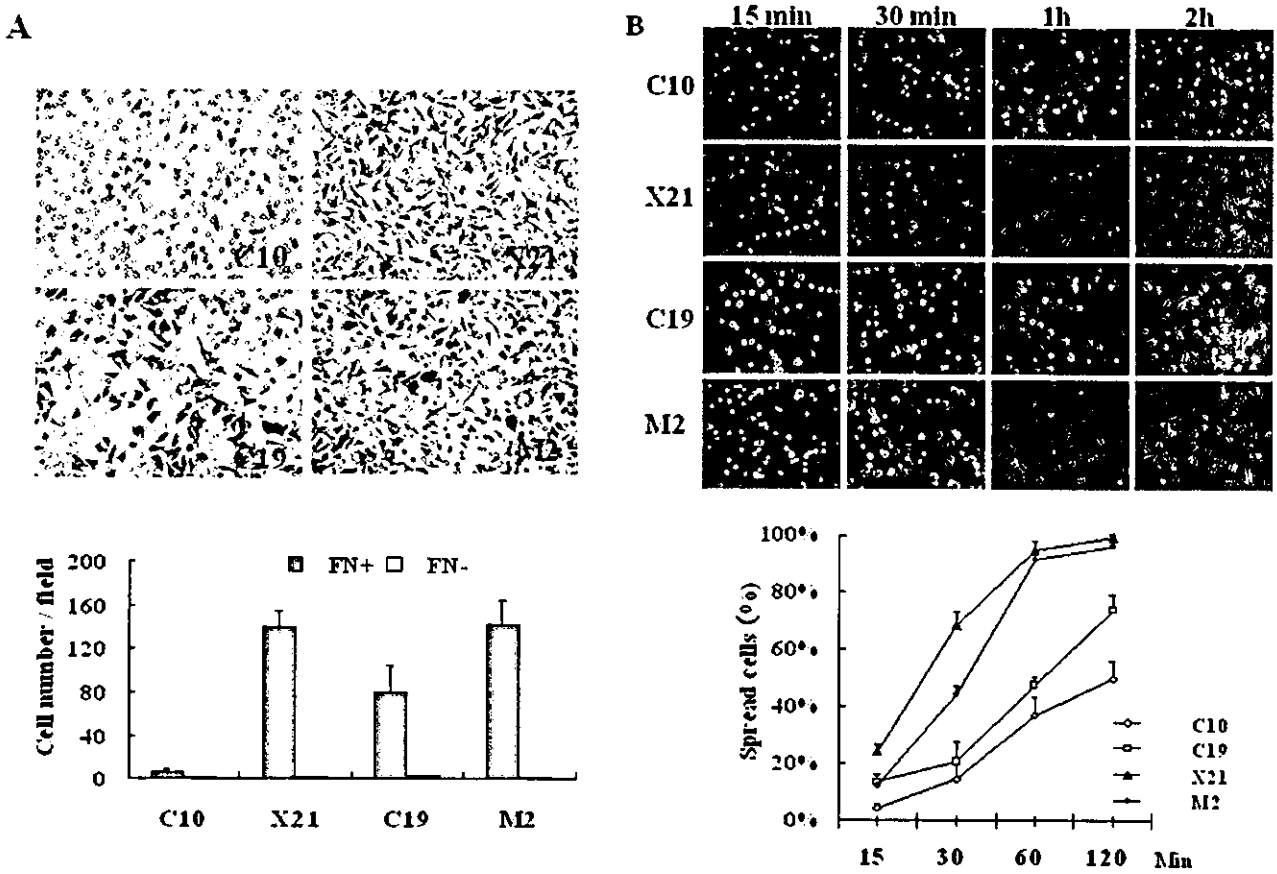

FIG. 1. **Enhanced motility and spreading ability on FN in highly metastatic murine melanoma cell lines.** *A*, cell motility under FN stimulation was elevated in highly metastatic cells. Haptotactic cell migration toward FN was measured using modified Boyden chamber cell migration assay as described under "Experimental Procedures." Cells migrated through the filter in 3 h and spread on the lower side of the filter were fixed, exposed to Giemsa staining, and visualized by a microscope at a magnification of 200×. The number of cells was counted from at least eight microscope fields. The *error bars* show the standard deviation. *B*, enhanced cell spreading ability of highly metastatic cells. A cell spreading assay was carried out as described under "Experimental Procedures." 10^5/ml cells in DMEM containing 0.5% FCS were plated on FN-coated dishes (10 μg/ml). Photos of cells were taken under the microscope at a magnification of 200× at the indicated times. Single cells that were phase bright with rounded morphology were scored as nonspread, whereas those that possessed a flat shape and were phase dark were scored as spread. The percentages of spread cells at each time point were scored as indicated. The same experiment was repeated at least three times, and the *error bars* show the standard deviation.

3Y1-Crk is an isolated clone of rat 3Y1 cells transfected with v-Crk cDNA of an avian sarcoma virus CT10 inserted in expression vector pMV-7. 3Y1-Vec is an isolated clone of rat 3Y1 cells transfected with expression vector pMV-7 (16). All tumor cells were maintained in Dulbecco's modified Eagle's medium (DMEM[1]; Sigma) supplemented with 10% fetal calf serum (FCS; Sigma) and grown in the presence of penicillin and streptomycin (Sigma) at 37 °C with 5% CO_2.

Antibodies and Reagents—Polyclonal antibodies against Src family tyrosine kinase (Src-2), Src (Src-N-16), or Fyn (Fyn3) were obtained from Santa Cruz Biotechnology. Anti-phosphotyrosine antibody 4G10, polyclonal antibody against human Fyn, and monoclonal antibody against cortactin (clone 4F11) were obtained from Upstate Biotechnology, Inc. Monoclonal antibodies against Yes, Hck, or FAK were obtained from Transductory Laboratories. Monoclonal antibody against paxillin was obtained from Zymed Laboratories Inc. Polyclonal antibodies against Cas (Cas3 and Cas2) were used as described previously (16). Rhodamine-labeled phalloidin was purchased from Molecular Probes, and fluorescein isothiocyanate-conjugated anti-mouse and rhodamine-conjugated anti-rabbit antibodies were obtained from Santa Cruz Biotechnology. Polylysine, fibronectin, and cycloheximide were purchased from Sigma. Src family kinases inhibitor 4-amino-5-(4-chlorophenyl)-7-(t-butyl)pyrazolo[3,4-d]pyrimidine (PP2) and the structural analog 4-amino-7-phenylpyrazol [3,4-d]pyrimidine (PP3) were obtained from Calbiochem-Novabiochem Ltd.

Cell Stimulation with Fibronectin or Polylysine—The cells were serum-starved (on dish) in DMEM containing 0.5% FCS for 18 h, washed by phosphate-buffered saline (PBS), and harvested by trypsin-EDTA treatment (0.5% trypsin, 2 mM EDTA) in DMEM. The trypsin was inactivated by the addition of soybean trypsin inhibitor (0.5 mg/ml) (Sigma), and the cells were collected by centrifugation, resuspended in DMEM containing 0.5% FCS, and held in suspension for 30 min at 37 °C (off dish). The cell culture dishes were precoated with FN purified from bovine plasma (10 μg/ml) or polylysine (10 μg/ml) (Sigma) in PBS overnight at 4 °C, rinsed with PBS, and warmed to 37 °C for 1 h. Suspended cells were distributed onto ligand-coated dishes and incubated at 37 °C. At various times following plating as indicated, the attached cells were rinsed in PBS and lysed in 1% Triton X-100 buffer (see below). Total cell proteins in lysates were standardized prior to use.

Cell Lysis, Immunoblotting, and Immunoprecipitation—Protein extraction and Western blotting analysis were performed as described (6). Briefly, the cells were lysed in 1% Triton X-100 buffer (50 mM Hepes, 150 mM NaCl, 10% glycerol, 1% Triton X-100, 1.5 mM $MgCl_2$, 1 mM EGTA, 100 mM NaF, 1 mM Na_3VO_4, 10 μg/ml approtinin, 10 μg/ml leupeptin, 1 mM phenylmethylsulfonyl), and insoluble material was removed by centrifugation. The protein aliquots were separated by SDS-PAGE and probed with 1:2000 diluted antibodies. For immunoprecipitation, 500 μg of protein was mixed with 1–2 μg of antibodies against cortactin, Src family (Src-2), Src (Src-N-16), Fyn, Cas3, paxillin, or FAK and incubated for 1 h on ice. Then samples were rotated with

[1] The abbreviations used are: DMEM, Dulbecco's modified Eagle's medium; FCS, fetal calf serum; PP2, 4-amino-5-(4-chlorophenyl)-7-(t-butyl)pyrazolo[3,4-d]pyrimidine; PP3, 4-amino-7-phenylpyrazol [3,4-d]pyrimidine; FN, fibronectin; PBS, phosphate-buffered saline; CHX, cycloheximide.

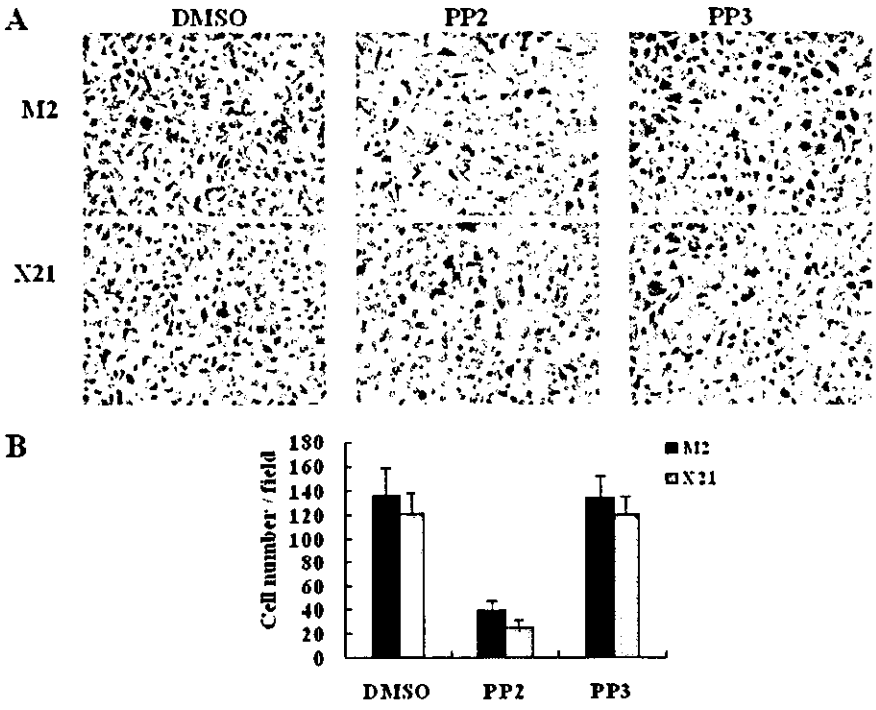

FIG. 2. **Impaired cell motility by PP2 treatment in highly metastatic murine melanoma cells.** The cells were subjected to haptotactic cell migration toward FN using a Boyden chamber in the presence of PP2 (10 μM), dimethyl sulfoxide (*DMSO*, 10 μM), or PP3 (10 μM) in the upper well as described under "Experimental Procedures." The cells were allowed to move in 3 h toward FN added to the lower chamber; the cells at the lower side of the filter were exposed to Giemsa staining and visualized under microscope at a magnification of 200×. The number of cells on the lower side of the filter was counted from at least eight fields (*error bars* show the standard deviation). The results presented here are representative mean values of experiments performed four times.

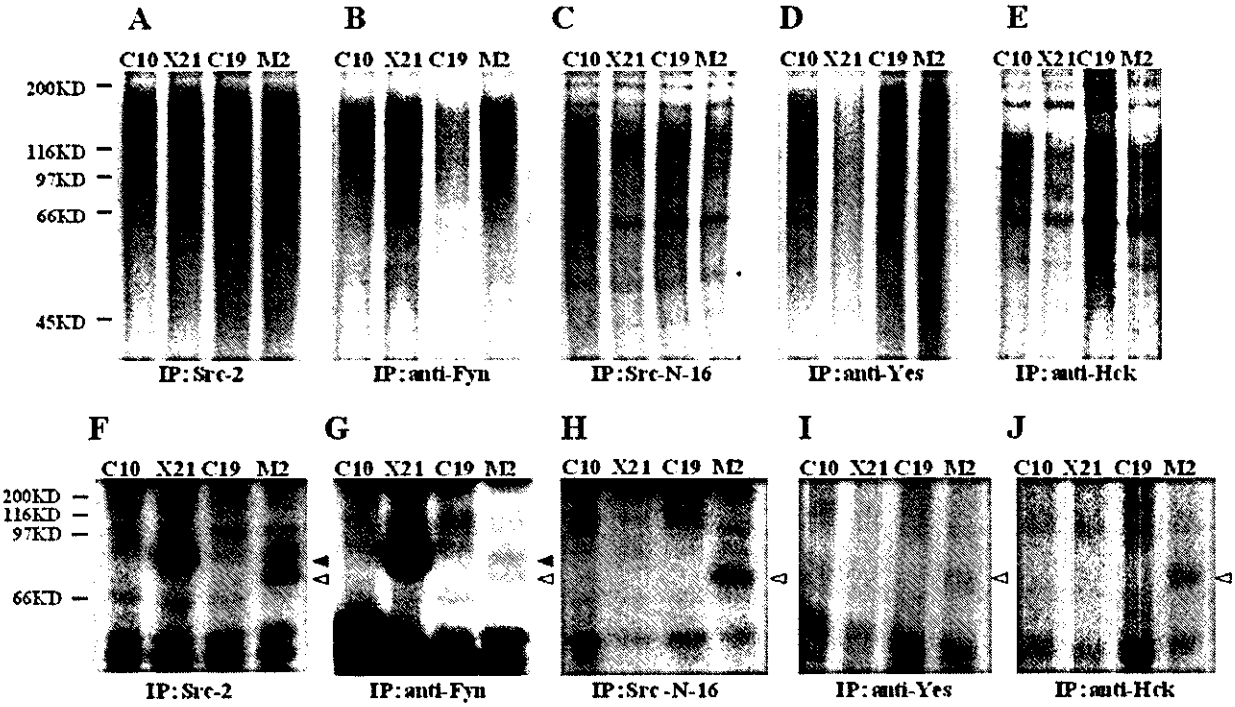

FIG. 3. **Elevated Fyn kinase activity and highly phosphorylated proteins associated with Fyn in cells with high metastatic potential.** The cells plated on plastic culture dishes for 48 h were lysed using 1% Triton X-100 buffer as described under "Experimental Procedures." Src family kinases in equal portions of cell lysates were isolated by immunoprecipitation (*IP*) using antibodies against Src family (Src2; *A* and *F*), Fyn (*B* and *G*), Src (Src-N-16; *C* and *H*), Yes (*D* and *I*), or Hck (*E* and *J*). The immunoprecipitates were labeled by [γ-^{32}P]ATP in an *in vitro* kinase assay in the presence (*A–E*) or absence (*F–J*) of exogenous synthetic polypeptides poly[Glu-Tyr]. The labeled proteins were analyzed by SDS-PAGE and visualized by autoradiography. The results presented here are representatives of experiments performed at least twice. *A–E*, kinase activities of Src family kinases in the presence of poly[Glu-Tyr]. Elevated Fyn activity in X21 and M2 was observed. *F–J*, phosphorylated proteins associated with Src family kinases in mildly or highly metastatic cells in an *in vitro* kinase assay. Fyn-associated proteins with a size of 85 kDa were specially observed in X21 and M2 (as indicated by *closed triangles*). Phosphorylated proteins with a size of 80 kDa in M2 associated with Src, Yes, and Hck in M2 are indicated by *open triangles*.

protein A- or protein G-Sepharose beads (Sigma) for 1 h at 4 °C. The beads were washed four times with 1% Triton X-100 buffer and boiled in sample buffer (2% SDS, 0.1 M Tris-HCl, pH 6.8, 10% glycerol, 0.01% bromphenol blue, 0.1 M dithiothreitol) before being subjected to SDS-PAGE analysis.

Immunofluorescence—Immunofluorescence staining was performed

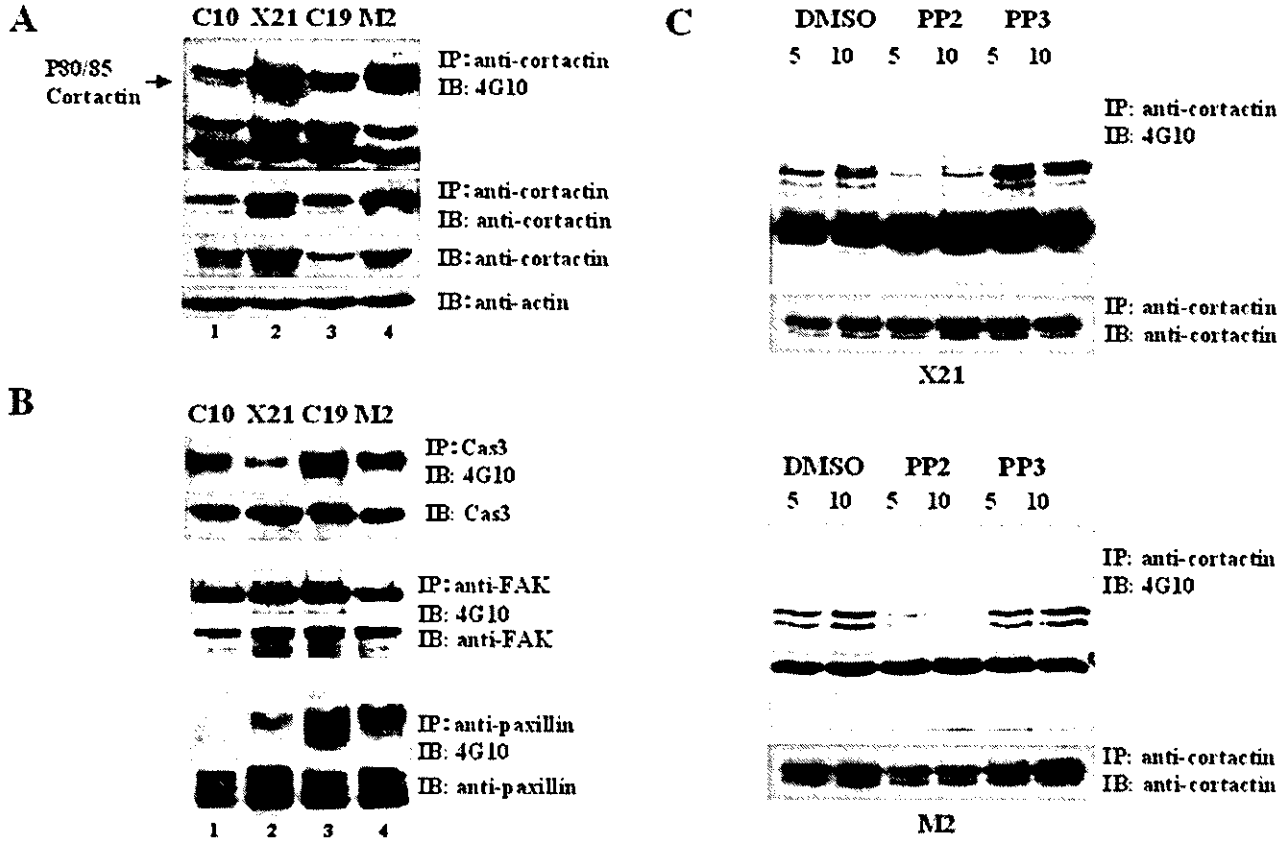

FIG. 4. **Overexpression and hyperphosphorylation of cortactin in cells with high metastatic potential.** Cells plated on plastic culture dishes for 48 h were lysed in 1% Triton X-100 buffer as described under "Experimental Procedures." Tyrosine phosphorylation of cortactin, $p130^{Cas}$, paxillin, and FAK in equal portions of cell lysates were analyzed by immunoprecipitation (*IP*) using antibody against cortactin (UBI), $p130^{Cas}$, paxillin (Zymed Laboratories Inc.), or FAK (Transduction Laboratories). The immunoprecipitates were subjected to immunoblotting analysis by anti-phosphotyrosine antibody 4G10. As a control, quantity of cortactin, $p130^{Cas}$, paxillin, or FAK in equal amount of whole cell lysates were also analyzed by immunoblotting (*IB*). *A*, expression and tyrosine phosphorylation of cortactin are up-regulated in highly metastatic cells X21 and M2. *B*, expression and tyrosine phosphorylation of $p130^{Cas}$, paxillin, and FAK in melanoma cells. *C*, PP2 treatment impaired tyrosine phosphorylation of cortactin in highly metastatic cell lines X21 (*upper panel*) and M2 (*lower panel*). The cells cultured in DMEM with 10% FCS were washed by DMEM and then treated by PP2 (10 μM), Me_2SO (10 μM), or PP3 (10 μM) in DMEM for 15 min before being lysed in 1% Triton X-100 buffer. Cortactin in equal portions of cell lysates was isolated by immunoprecipitation and subjected to immunoblotting by anti-phosphotyrosine antibody 4G10.

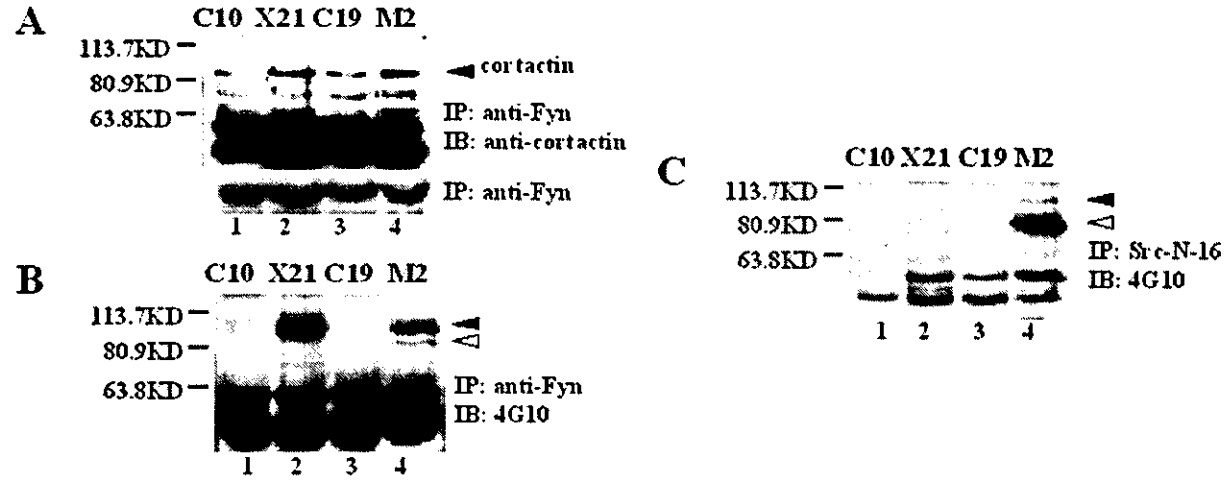

FIG. 5. **Specific association between cortactin and Fyn in highly metastatic melanoma cells.** *A*, physical association between cortactin and Fyn. Equal amounts of immunoprecipitates (*IP*) by antibody against Fyn (Fyn3) (Santa Cruz Biotechnology) were subjected to immunoblotting (*IB*) by anti-cortactin antibody. The expression of Fyn was indicated by immunoblotting analysis of equal amount of whole cell lysates using antibody against Fyn (Fyn3). Enhanced association between cortactin and Fyn in X21 and M2 were observed. *B* and *C*, tyrosine-phosphorylated proteins associated with Fyn (*B*) or Src (*C*) were analyzed by immunoblotting equal portion of immunoprecipitations against Fyn or Src (Src-N-16, Santa Cruz Biotechnology) with anti-phosphotyrosine antibody 4G10 (UBI). Tyrosine phosphorylation of Fyn-associated protein with a size of 85 kDa (indicated by *closed triangle*) in X21 and M2 and tyrosine phosphorylation of Src-associated protein in M2 with a size of 80 kDa (indicated by *open triangle*) were observed.

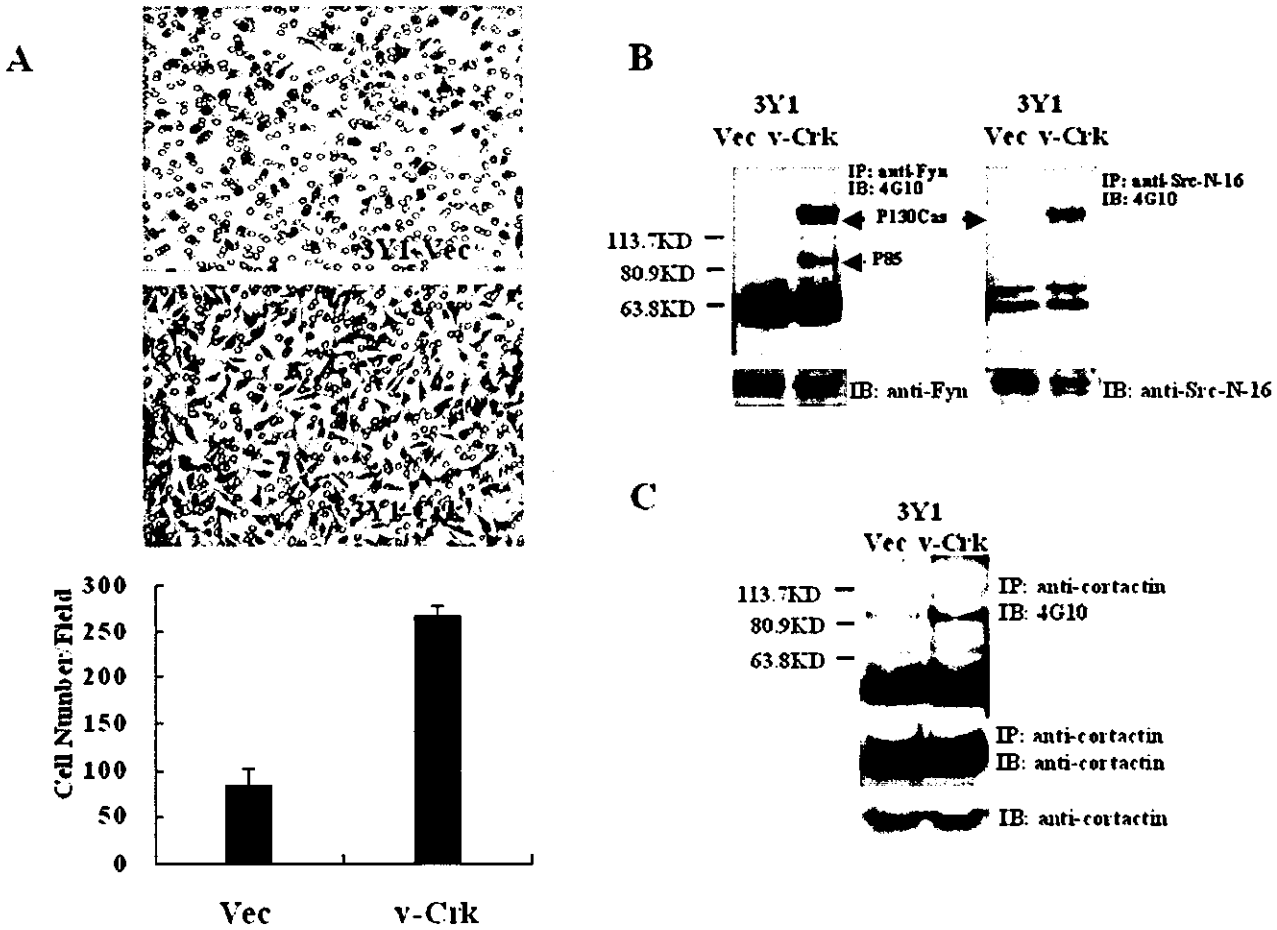

FIG. 6. **Fyn-cortactin association in 3Y1-Crk fibroblasts.** *A*, cell motility was enhanced in 3Y1-Crk fibroblasts. A modified Boyden chamber cell migration assay was performed as described under "Experimental Procedures." The cells that had migrated through the filter were fixed, exposed to Giemsa staining, and visualized by a microscope at a magnification of 200×. The number of cells on the lower side of the filter was counted from at least eight fields (*error bars* show the standard deviation). The results presented here are representative mean values of experiments performed three times. *B*, tyrosine-phosphorylated proteins $p130^{Cas}$ and P85 were associated with Fyn in 3Y1-Crk fibroblasts. *C*, elevated tyrosine phosphorylation of cortactin in 3Y1-Crk fibroblasts. Fyn-associated tyrosine-phosphorylated protein and phosphotyrosine of cortactin in 3Y1-Crk fibroblasts were determined by immunoblotting equal portion of immunoprecipitations (*IP*) against Fyn or cortactin (UBI) with anti-phosphotyrosine antibody 4G10 (UBI). The quantity of Fyn or cortactin in an equal amount of whole cell lysates was also analyzed by immunoblotting (*IB*).

essentially as described previously (6). 6×10^4 cells were plated onto 12-mm circle cover glasses (Fisher), which were placed in each well of a 24-well plate and allowed to grow for 24 h in DMEM with 10% FCS at 37 °C with 5% CO_2. Where necessary, the 12-mm circle cover glasses were coated with FN (10 μg/ml) or polylysine (10 μg/ml) overnight in PBS, respectively, before cells plating. The cells were then fixed with 4% paraformaldehyde in 0.1 M sodium phosphate (pH 7.0) for 5 min, washed three times with PBS, and permeabilized with 0.1% Triton X-PBS for 10 min before blocking with 2% bovine serum albumin with TBST (0.15 M NaCl, 1% Tris, pH 7.0, 0.05% Tween 20). Then the cells were incubated with the first antibody anti-cortactin (5 ng/μl) or anti-Fyn (Fyn3) (5 ng/μl) in 2% bovine serum albumin with TBST to stain cortactin or Fyn for 1 h. After washing three times with PBS, the cells were then incubated with fluorescein isothiocyanate-conjugated anti-mouse IgG antibody (1:40) or rhodamine-conjugated anti-rabbit IgG antibody (1:40) for 30 min. In staining actin stress fibers, the cells were incubated with rhodamine-conjugated phalloidin (1:200, 1 unit/ml) for 30 min in 2% bovine serum albumin with TBST. After the cells were washed three times with PBS, the cover glasses were mounted in a 1:1 mixture of 2.5% DABCO (Sigma) in PBS and glycerol. The cells were then visualized using a Radiance 2100 confocal microscopic system (Bio-Rad).

Cell Migration Assay—Cell motility of 3Y1-Crk fibroblasts was performed as described previously (6). Haptotactic cell migration of all the melanoma cells was analyzed using Boyden chamber cell migration assay with some modification. The conditions are described in a previous study (17). In detail, the cells were trypsinized, washed once in DMEM with 10% FCS, and washed once in serum-free DMEM. 1.5×10^6 cells were then resuspended to 560 μl of DMEM with 15 mM Hepes buffer (pH 7.2) and added to the upper well of the Boyden chamber. To investigate the effect of PP2 treatment on cell motility, the cells were added to the upper well under the same conditions in the presence of PP2 (10 μM), Me_2SO (10 μM), or PP3 (10 μM). FN (Sigma) was diluted in 1280 μl of medium as described above at a concentration of 10 μg/ml and filled the lower well of the chamber. A polyvinylpyrrolidone-free polycarbonate filter with an 8-μm pore size (Neuroprobe) was used. The chamber containing the cells was incubated for 3 h at 37 °C in a humid 5% CO_2 atmosphere. The cells at the lower surface of the filter were fixed in methanol for 30 min, washed with PBS, and then exposed to Giemsa staining for 15 s. After washing three times with PBS, the filter was mounted on a glass slide. The side of the filter to which cells had been added was scraped. The number of migrated cells was counted from photographs taken of at least eight fields at a magnification of 200× under the microscope.

Cell Spreading Assay—Cells in confluence were overnight serum-starved, harvested with 0.5% trypsin and 2 mM EDTA, and washed once with soybean trypsin inhibitor (0.5 mg/ml) in DMEM before being resuspended with DMEM at 10^5 cells/ml. The cells were then plated on dishes coated with FN (10 μg/ml) (Sigma). Photos of cells were taken at the indicated times. Single cells that were phase bright with rounded morphology were scored as nonspread, whereas those that possessed a flat shape and were phase dark were scored as spread. The percentage of spread cells was calculated by counting the spread cells in

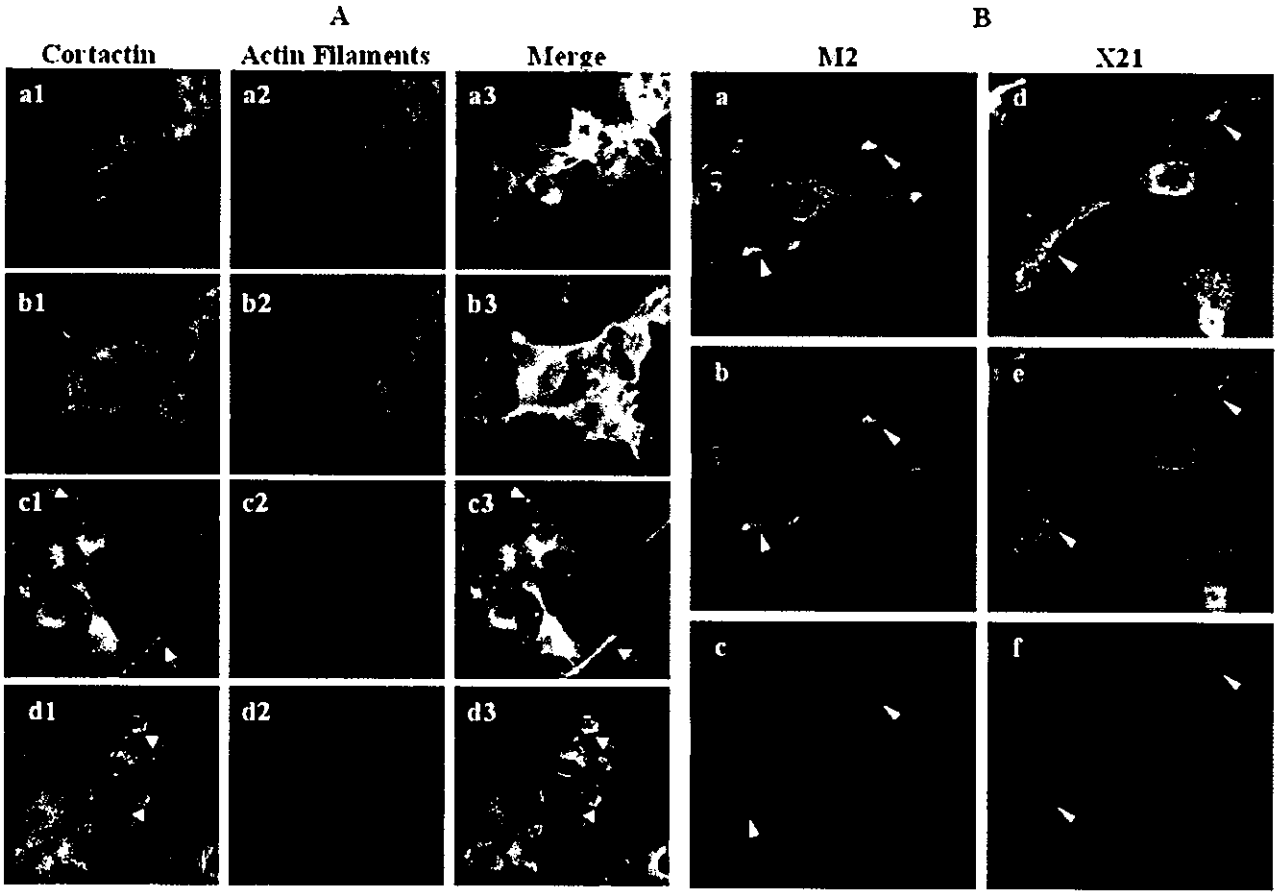

FIG. 7. **Subcellular co-localization of cortactin with actin filaments or Fyn in melanoma cells with high metastatic potential.** Co-localizations of cortactin and actin filaments (*A*) or co-localizations of cortactin and Fyn (*B*) in melanoma cell lines were investigated by immunofluorescence staining. The cells plated on 12-mm circle cover glasses were allowed to grow for 24 h in DMEM with 10% FCS at 37 °C with 5% CO_2, then fixed, permeabilized, and stained by primary antibody against cortactin (UBI) and rhodamine-conjugated phalloidin (Molecular Probes) or Fyn (Fyn3) (Santa Cruz Biotechnology) (10 ng/μl). Fluorescein isothiocyanate-conjugated anti-mouse IgG or rhodamine-conjugated anti-rabbit IgG antibody (Santa Cruz Biotechnology) were utilized as secondary antibodies. The cells were then visualized by a Radiance 2100 confocal microscopic system (Bio-Rad). *A*, co-localizations of cortactin and actin filaments in C10 (*panels a1*, *a2*, and *a3*), C19 (*panels b1*, *b2*, and *b3*), X21(*panels c1*, *c2*, and *c3*), and M2 (*panels d1*, *d2*, and *d3*). Co-localizations of cortactin and actin filaments at membrane protrusions or extensions are indicated by *arrowheads*. *B*, co-localizations of cortactin and Fyn in membrane protrusions or extensions in M2 and X21. The triangles indicate co-localizations of cortactin and Fyn. *Panels a–c*, M2; *panels d–f*, X21. *Panels a* and *d*, merged localization of cortactin and Fyn; *panels b* and *e*, anti-cortactin; *panels c* and *f*, anti-Fyn.

each microscope field. The same experiment was repeated at least three times.

Immune Complex Kinase Assay—For immune complex assay, each member of Src family kinases in cell lysates containing 500 μg of proteins was first immunoprecipitated by antibody against Fyn (UBI), Src family (Src2), Src (Src-N-16) (Santa Cruz Biotechnology), Yes, or Hck (Transduction Laboratories). Then immunoprecipitates were consequently washed using 1% Triton buffer and kinase buffer (50 mM Tris, pH 7.4, 50 mM NaCl, 10 mM $MgCl_2$, 10 mM $MnCl_2$) three times, respectively. To each sample, 1 μl of exogenous synthetic polypeptides poly-[Glu-Tyr] was added as exogenous substrate. Kinase reaction was performed in 30 μl of kinase buffer with 5 μCi of [γ-^{32}P]ATP (ICN) at room temperature for 30 min. Kinase reactions were stopped by the addition of SDS-PAGE sample buffer (2% SDS, 0.1 M Tris, pH 6.8, 10% glycerol, 0.01% bromphenol blue, 0.1 M dithiothreitol). The samples were then subjected to SDS-PAGE analysis using 8% polyacrylamide gel. The gels were then dried and exposed to autoradiography.

RESULTS

Highly Metastatic Murine Melanoma Cell Lines Exhibited Enhanced Motility and Spreading Ability on Fibronectin—To clarify differences in cell properties that correspond to the diversity of metastatic potentials of K-1735 cell lines, we measured haptotactic cell migration ability toward FN using a Boyden chamber. As shown in Fig. 1*A*, about 140 cells/field of highly metastatic cells X21 and M2 migrated through the pores of the filter in 3 h toward FN. In contrast, for low metastatic cells C19 and C10, only about 70 cells/field of C19 and no more than 10 cells/field of C10 migrated through the pores toward FN, respectively. No cell locomotion was observed in the absence of FN in any of these cell lines, suggesting that these cells exhibit FN-dependent cell motility. Cell motility under the stimulation of integrin correlates with metastatic potentials. To determine their differences in spreading abilities, time-dependent cell spreading was estimated by the percentage of flat cells in all of cells at attachment after plating on FN-coated dishes (see "Experimental Procedures"). About 70% of X21 and 45% of M2 exhibited a flat shape with multiple protrusions 30 min after plating on FN. In contrast, about 20% of C19 and 17% of C10 were spread (Fig. 1*B*). After plating on FN for 60 min, the percentages of flat cells of X21 and M2 increased to about 98%, whereas there were less than 50% C19 and C10 showing a flat shape (Fig. 1*B*). These results demonstrate that cell spreading of X21 and M2 occurs much faster than that of C10 and C19. Both cell migration and cell spreading abilities were enhanced in highly metastatic cell lines.

Analysis of Src Family Kinases Responsible for Enhanced Cell Motility of Melanoma Cells with High Metastatic Potential—Roles of Src family tyrosine kinases in cell migration of

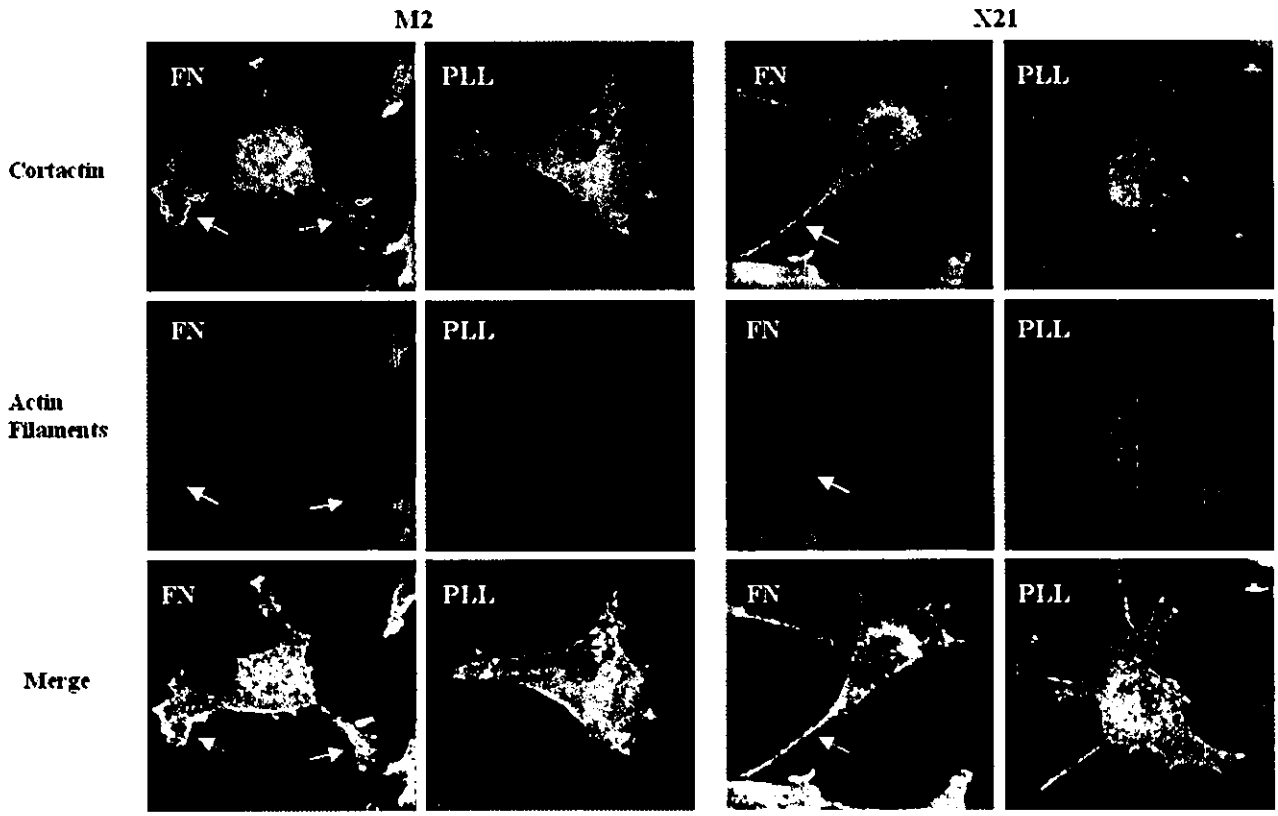

FIG. 8. **Integrin stimulated redistributions of cortactin with actin filaments in highly metastatic cells.** M2 and X21 cells were plated onto 12-mm circle cover glasses (Fisher Scientific), which were coated with FN (10 μg/ml) or polylysine (*PLL*, 10 μg/ml), overnight in PBS and allowed to grow for 24 h in DMEM with 1% FCS at 37 °C with 5% CO_2. Then co-localization of cortactin and actin filaments in highly metastatic melanoma cell lines was investigated by immunofluorescence staining using rhodamine-conjugated phalloidin (Molecular Probes) or antibody against cortactin (UBI) and fluorescein isothiocyanate-conjugated anti-mouse IgG (1:40). The cells were then visualized by a Radiance 2100 confocal microscopic system (Bio-Rad). Redistribution of cortactin co-localized with actin filaments at lamellipodias in M2 or fillopodias in X21 on FN were observed in merged images (as indicated by *arrows*).

X21 and M2 cells were investigated by the Boyden chamber in the presence of specific inhibitor of Src family kinases including Src, Fyn and Hck, PP2 (18). The inactive structural analog PP3 and Me_2SO were used as negative controls. Treatment of PP2 significantly reduced the number of cells migrating through the pores in 3 h from 140 to about 30/field (Fig. 2), whereas negative controls Me_2SO or PP3 did not show such an effect, showing that PP2 impairs cell motility of X21 and M2. These results demonstrate that some member(s) of Src family kinases play essential roles in cell migration of highly metastatic cells.

To characterize the member of the Src kinases responsible for the enhanced cell motility and spreading ability detected in highly metastatic cells M2 and X21, the kinase activities of Src, Fyn, Yes, and Hck were investigated using an *in vitro* immune complex kinase assay in the presence of exogenous synthetic polypeptides poly[Glu-Tyr] as substrates. No significant differences in kinase activities of Src and Yes were observed in any of the cell lines with different metastatic potentials (Fig. 3, *C* and *D*). In the case of Hck, the kinase activity was rather lower in X21 and M2 (Fig. 3*E*), whereas the activity of Fyn was particularly elevated in highly metastatic cells X21 and M2 compared with C10 and C19 (Fig. 3*B*). These results indicate that Fyn is a candidate Src family kinase responsible for high metastatic potential in X21 and M2 melanoma cells.

In the absence of exogenous substrate, a distinct 85-kDa protein was significantly phosphorylated by the immune complex kinase assay by pan-Src and Fyn in X21 and M2 (Fig. 3, *F* and *G*, *closed triangles*) but not in C10 or C19. This protein was not detected in protein complexes immunoprecipitated by Src (Src-N-16), Yes, or Hck (Fig. 3, *H–J*), demonstrating that this protein is specifically associated with Fyn in highly metastatic cell lines. An 80-kDa phosphorylated band was also immunoprecipitated by Src, Hck, or Yes only in M2 (Fig. 3, *H–J*, *open triangles*). Judging from differences in molecular size and substrate specificity, this protein is distinct from the 85-kDa protein observed in both X21 and M2.

Overexpressed and Hyperphosphorylated Cortactin Was Specifically Associated with Fyn in Highly Metastatic Cells—Cortactin, a protein of 80/85 kDa, acts as a potential linker between membrane-located receptors and cytoskeleton, primarily affecting cell motility and invasion (11–13). Because the molecular size of cortactin appeared close to the size of the protein associated with Fyn in X21 and M2 (Fig. 3*G*), we examined the expression and tyrosine phosphorylation of cortactin in these murine melanoma cells. As expected, tyrosine phosphorylation of cortactin was significantly elevated in X21 and M2 (Fig. 4*A*, *lanes 2* and *4*) compared with that of C10 and C19 (Fig. 4*A*, *lanes 1* and *3*). Expression levels of cortactin in X21 and M2 were also up-regulated (Fig. 4*B*, *lanes 1* and *3*). Tyrosine phosphorylation levels of cortactin were much reduced by Src family kinase inhibitor PP2 in X21 and M2 in contrast to PP3 (Fig. 4*C*), confirming that Src family kinases are responsible for tyrosine phosphorylation of cortactin in X21 and M2. At the same time, we investigated the expression and tyrosine phosphorylation of other substrates of Src family kinases such as $p130^{Cas}$, FAK, and paxillin. As shown in Fig. 4*B*, tyrosine phosphorylation of $p130^{Cas}$ was reduced in X21 and M2 compared with that in C10 and C19, and no significant differences

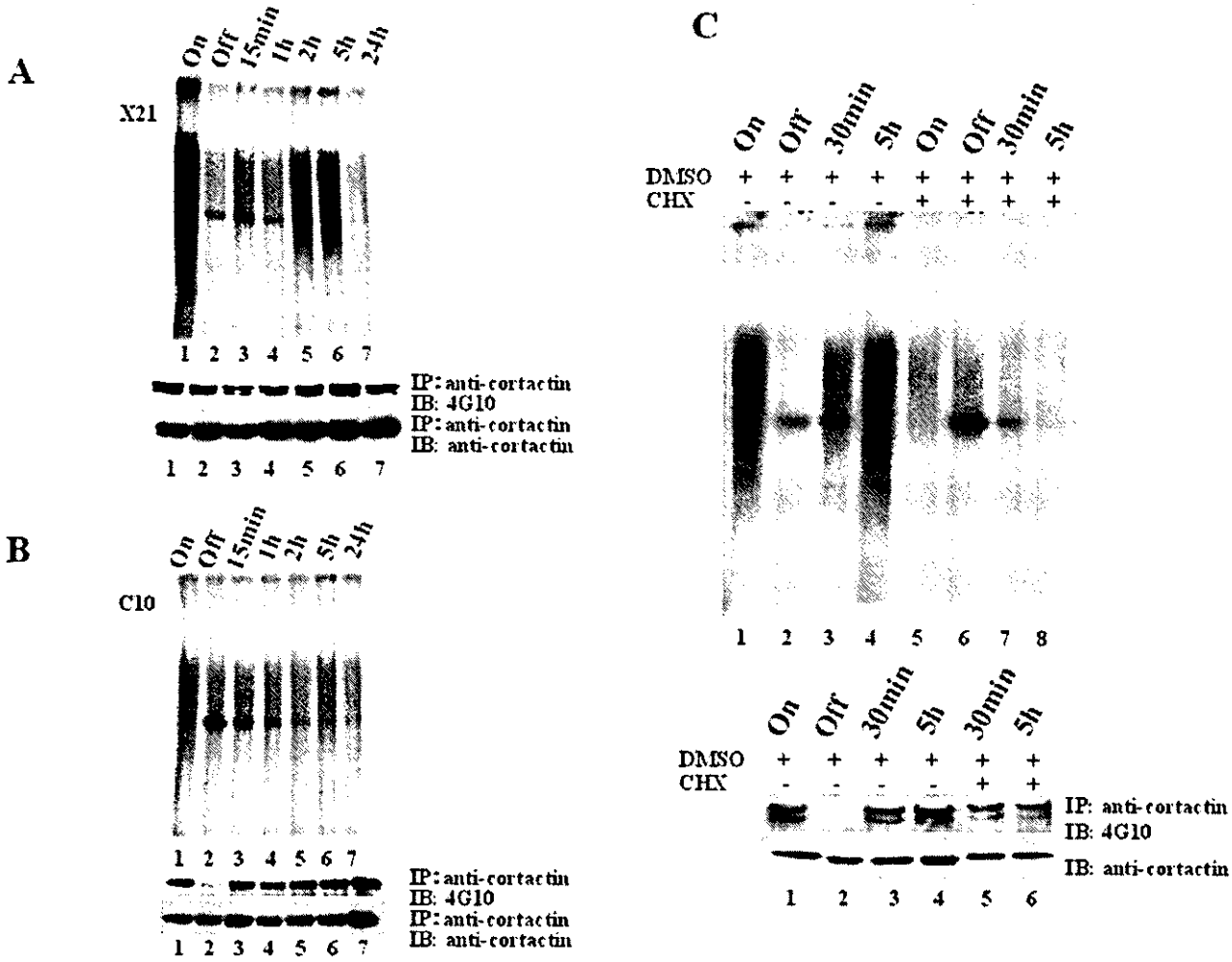

FIG. 9. **Late phase activation of Fyn under integrin stimulation in cells with high metastatic potential.** The cells were either serum-starved (on dish), held in suspension for 30 min (off dish), or plated onto FN-coated dishes for the times indicated. Fyn in equal portions of cell lysates were isolated by immunoprecipitation (*IP*) using antibodies against Fyn (UBI), and the immunoprecipitates were labeled by [γ-^{32}P]ATP in an *in vitro* kinase assay in the presence of exogenous synthetic polypeptides poly[Glu-Tyr]. The labeled proteins were analyzed by SDS-PAGE and visualized by autoradiography. Tyrosine phosphorylation of cortactin in equal cell lysates were also analyzed by immunoprecipitation using antibody against cortactin and immunoblotting (*IB*) by tyrosine phosphorylation antibody 4G10. The results presented here are representative of experiments performed at least twice. *A*, integrin-stimulated Fyn activation (*upper panel*) and tyrosine phosphorylation of cortactin (*lower panel*) exhibited a peak at 2–5 h after plating in X21. *B*, no peak of Fyn activation and tyrosine phosphorylation of cortactin under integrin stimulation in C10 was observed. *C*, effects of cycloheximide on integrin-induced activation of Fyn (*upper panel*) and tyrosine phosphorylation of cortactin (*lower panel*). The cells were either serum-starved, held in suspension for 30 min, or plated onto FN-coated dishes for the times indicated in the absence (*lanes 1–4*) or presence (*upper panel, lanes 5–8; lower panel, lanes 5* and *6*) of cycloheximide (10 μg/ml) (Sigma). Then *in vitro* kinases assay was carried out in the presence of poly[Glu-Tyr] as described above.

of FAK tyrosine phosphorylation were detected among these cells. Tyrosine phosphorylation and expression of paxillin in C10 were much lower, but they were at the same level in C19 as in X21 and M2. Cortactin was the only phosphotyrosine-containing protein showing significantly elevated phosphorylation levels in highly metastatic cell lines.

Further study confirmed that cortactin was specifically associated with Fyn in X21 and M2. It was observed that the amount of cortactin coupling with Fyn in X21 and M2 was significantly greater than that in C10 and C19 (Fig. 5*A*). Correspondingly, tyrosine phosphorylation of the protein with a size of 85 kDa associated with Fyn in X21 and M2 was also observed (Fig. 5*B*, *lanes 2* and *4*). In contrast, an 80-kDa tyrosine-phosphorylated protein associated with Src was only observed in M2 but not in X21 (Fig. 5*C*, *lane 4*). This M2-specific protein was later identified as a *gag* protein derived from murine mammary tumor virus by means of mass spectrometry analysis,[2] which might be infected during the establishment of the M2 cell line by *in vivo* selection. There has been no report on tyrosine phosphorylation of this protein so far, and its roles on the metastatic potential of M2 are currently under investigation.

To provide additional evidence for essential roles of kinase-substrate cooperation between Fyn and cortactin, v-Crk transformed 3Y1 fibroblasts were used in which Fyn was reported to be activated by v-Crk (19). Following Fyn activation, elevated cell motility was observed in 3Y1-Crk cells compared with mock-transfected 3Y1-vec cells as shown in Fig. 6*A*. At the same time, tyrosine phosphorylation of cortactin was significantly enhanced in 3Y1-Crk fibroblasts (Fig. 6*C*), and the same molecular sizes of phosphoproteins were obvious among Fyn-associated phosphoproteins apart from p130^{Cas}, which has

[2] J. Huang, T. Asawa, T. Takato, and R. Sakai, unpublished data.

been reported to be associated with Fyn (Fig. 6*B*). These results in fibroblasts also support the possibility that cortactin tyrosine phosphorylation is regulated by Fyn in relation to signaling of cell migration.

Subcellular Localization of Fyn and Cortactin in Melanoma Cell Lines—Because cortactin has been functionally identified as an actin-associated protein (20–22), we also investigated co-localizations of cortactin with actin in C10, C19, X21, and M2. First, different distribution patterns of actin filaments between low and highly metastatic cells were noticed on non-coated glass slides. Significantly increased amounts of actin filaments were found at cell membrane protrusions in highly metastatic cells X21 and M2 (Fig. 7*A*, *panels c2* and *d2*). In contrast, actin filaments were widely (nonspecifically) observed in cell matrix in C10 and C19 (Fig. 7*A*, *panels a2* and *b2*). It was also observed that overexpressed cortactin was localized in these cell membrane protrusions specific to X21 and M2 (Fig. 7*A*, *panels c1*, *d1*, *c3*, and *d3*), implying that cortactin is associated with signaling of actin cytoskeleton organization near the membrane in highly metastatic cells. Results of staining of Fyn and cortactin demonstrated that most of cortactin and Fyn were distributed at cell membrane protrusions in M2 and X21 (Fig. 7*B*, *panels a* and *d*, *arrows*), showing apparent co-localization of cortactin and Fyn at these structures.

To further investigate the role of cortactin in highly metastatic cells, we explored co-localization of cortactin with actin filaments in X21 and M2 under the stimulation of integrin. As shown in Fig. 8, cortactin was co-localized with actin filaments at lamellipodias or fillopodias in M2 or X21, which were formed under the stimulation of FN.

Late Response of Fyn Activation by FN Requires de Novo Protein Synthesis—To illustrate molecular mechanisms underlying FN-stimulated redistribution of cortactin and formation of lamellipodia or fillopodia in highly metastatic cells X21 and M2, we explored the activity of Fyn under FN stimulation by *in vitro* kinase assay with poly[Glu-Tyr]. In X21, Fyn activity was relatively high when cells were at attachment (Fig. 9*A*, *lane 1*), whereas it was sharply reduced when cells were detached and kept in suspension for 30 min (Fig. 9*A*, *lane 2*). The activity of Fyn was restored 2 or 5 h after cells were plated on FN (Fig. 9*A*, *lanes 5* and *6*). Corresponding to the activation of Fyn, tyrosine phosphorylation of cortactin also exhibited a similar time course (Fig. 9*A*, *lower panel*). A similar pattern of activation of Fyn and tyrosine phosphorylation of cortactin by FN was also observed in M2.[2] In contrast, levels of Fyn activity were not significantly changed in C10 and C19 after each indicated time plated on FN (Fig. 9*B*).[2] Although tyrosine phosphorylation of cortactin was abolished by detachment, no obvious peaks in tyrosine phosphorylation of cortactin after each indicated time plated on FN were observed in these cells (Fig. 9*B*, *lower panel*). Preceding elevated Fyn activity at 2–5 h after stimulation, the expression level of cortactin was also increased from 1 to 2 h in X21 (Fig. 9*A*, *lower panel*). The same results were observed in M2.[2]

The late phase activation of Fyn demonstrated by both M2 and X21 on FN raised the possibility of yet unidentified regulatory mechanisms in integrin-mediated Fyn activation. To determine whether *de novo* synthesis of regulatory proteins in this process is required, we investigated Fyn activity in the presence of cycloheximide (CHX), a protein synthesis inhibitor. As expected, elevated expression of cortactin induced by integrin stimulation was antagonized by CHX at 5 h after plating (Fig. 9*C*, *lower panel*, *lane 6*). At the same time, it was observed that activation of Fyn was significantly blocked by the treatment of CHX at 5 h after plating (Fig. 9*C*, *upper panel*, *lane 8*) compared with the control (Fig. 9*C*, *upper panel*, *lane 4*). Tyrosine phosphorylation of cortactin was also down-regulated by CHX treatment (Fig. 9*C*, *lower panel*, *lane 6*). The same results were observed in M2.[2] These findings indicate that *de novo* protein synthesis is involved in the late phase activation of Fyn by FN stimulation.7

DISCUSSION

Previous studies have shown that Fyn is an essential regulator in integrin-mediated processes including actin cytoskeleton organization, cell migration, and adhesion in normal cells (23–25). A recent study also demonstrated that Fyn is prerequisite for normal keratinocyte migration and squamous carcinoma invasion (26). However, little is known regarding the functional roles of Fyn in tumor metastasis. In this study, in contrast to Src, Yes, and Hck, enhanced levels of Fyn activity and late phase activations of Fyn after stimulation by FN were observed in highly metastatic murine melanoma cell lines. Activated Fyn caused hyperphosphorylation of cortactin and formation of stable complex between Fyn and cortactin in these metastatic cell lines, indicating that Fyn and cortactin are key molecules in the integrin signaling pathway during the development of cancer metastasis.

Activation of Fyn by integrin signaling is mediated by many kinds of proteins involved in integrin signaling, which includes caveolin 1, tyrosine kinases, FAK, or receptor protein tyrosine phosphatase α (23, 25, 27). It has been observed in several studies that the activity of Src is enhanced 20–40 min following FN stimulation in NIH 3T3 fibroblasts (28–31). In this study, it was observed that Fyn activation occurs as late as 2–5 h after fibronectin stimulation in metastatic melanoma cell lines, and integrin-mediated activation of Fyn requires *de novo* protein synthesis. One possibility is that the up-regulation of cortactin that occurred approximately 1–2 h after stimulation is a primary event that triggers the activation of Fyn and phosphorylation of cortactin itself. As a special substrate associated with Fyn in metastatic cells, it is possible that cortactin regulates the activity of Fyn through physical associations to SH2 of Fyn. Another possibility is that a third molecule(s), which is specifically expressed in metastatic cell lines under stimulation of integrin, might regulate activation of Fyn, although this protein(s) has not been identified. In this paper, we do not demonstrate that cortactin is a direct substrate of Fyn kinase. According to a recent paper, tyrosine phosphorylation of cortactin occurs via activation of Rac1 by c-Src in C3H fibroblasts (38). Therefore, there is a possibility that cortactin phosphorylation by Fyn is regulated in a similar indirect manner in highly metastatic melanoma cell lines.

Cortactin was first identified as a p80/85-kDa v-Src substrate in chicken embryo cells transformed by v-Src oncogene (32). It was implicated in the progression of breast tumors through gene amplification at chromosome 11q13 (33). The importance of tyrosine phosphorylation of cortactin in metastasis was also implicated in a recent report (34). In this study, overexpression and enhanced tyrosine phosphorylation of cortactin in highly metastatic cells was observed, and it was also clarified that cortactin was specifically associated with Fyn in cells with high metastatic potential. When the activity of Fyn was inhibited by PP2, tyrosine phosphorylation of cortactin was also down-regulated. Moreover, corresponding to up-regulated membrane redistribution of cortactin, co-localized cortactin and Fyn at cell membrane protrusions in highly metastatic cells were also observed. Taken together, these results indicate that cortactin is associated with Fyn in integrin-mediated signaling processes in cancer metastasis. Previous reports have shown that cortactin is primarily localized within peripheral cell structures such as lamellipodia, pseudopodia, and membrane ruffles and has been suggested to operate as a potential

linker between membrane-located receptors and cytoskeleton, primarily affecting cell motility and invasion (11, 12). In this study, corresponding to enhanced cell motility, co-localized cortactin with actin filaments at lamellipodias or fillopodias was also observed in highly metastatic cells. Studies in normal cells have shown that cortactin was actively involved in lamellipodia actin polymerization (20–22). Lamellipodias and fillopodias are membrane structures formed during cell spreading and migration (35). It can be deduced from these reports that cortactin plays important roles in cell migration through its roles in integrin-stimulated actin cytoskeleton rearrangements during cancer metastasis. Support for this deduction is provided by the study of overexpression of cortactin in human tumors or NIH 3T3 fibroblasts, which has been shown to result in increased cell motility (36, 37). Overall, results in this study indicate that the Fyn-cortactin pathway is specifically activated for signaling of cell migration and spreading during the progression of cancer metastasis.

Identification of specific involvements of Fyn and cortactin in integrin signaling pathways in metastatic melanoma cell lines provided important information for the understanding of mechanisms underlying the progression of cancer metastasis. Further studies are necessary to elucidate what is produced *de novo* for the activation of Fyn and how it affects Fyn activity stimulated by integrin in metastasis. Moreover, to fully clarify their roles in metastasis and to provide further information for cancer therapy, the effect of blocking tyrosine phosphorylation of cortactin or suppressing expression of cortactin on the metastasis potential also needs to be further investigated.

Acknowledgments—We thank Dr. I. J. Fidler for kindly providing murine melanoma cell lines. We also thank Dr. I. Kitabayashi for mass spectrometry analysis.

REFERENCES

1. Bishop, J. M. (1987) *Science* **235,** 305–311
2. Fidler, I. J. (1990) *Cancer Res.* **50,** 6130–6138
3. Fincham, V. J., and Frame, M. C. (1998) *EMBO J.* **17,** 81–92
4. Cary, L. A., Klinghoffer, R. A., Sachsenmaier, C., and Cooper, J. A. (2002) *Mol. Cell. Biol.* **22,** 2427–2440
5. Boyer, B., Bourgeois, Y., and Poupon, M. F. (2002) *Oncogene* **21,** 2347–2356
6. Huang, J., Hamasaki, H., Nakamoto, T., Honda, H., Hirai, H., Saito, M., Takato, T., and Sakai, R. (2002) *J. Biol. Chem.* **277,** 27265–27272
7. LaVallee, T. M., Prudovsky, I. A., McMahon, G. A., Hu, X., and Maciag, T. (1998) *J. Cell Biol.* **141,** 1647–1658
8. Irby, R. B., Mao, W., Coppola, D., Kang, J., Loubeau, J. M., Trudeau, W., Karl, R., Fujita, D. J., Jove, R., and Yeatman, T. J. (1999) *Nat. Genet.* **21,** 187–190
9. Takayama, T., Mogi, Y., Kogawa, K., Yoshizaki, N., Muramatsu, H., Koike, K., Semba, K., Yamamoto, T., and Niitsu, Y. (1993) *Int. J. Cancer* **54,** 875–879
10. Schlaepfer, D. D., Hauck, C. R., and Sieg, D. J. (1999) *Prog. Biophys. Mol. Biol.* **71,** 435–478
11. Wu, H., and Parsons, J. T. (1993) *J. Cell Biol.* **120,** 1417–1426
12. van Damme, H., Brok, H., Schuuring-Scholtes, E., and Schuuring, E. (1997) *J. Biol. Chem.* **272,** 7374–7380
13. Huang, C., Liu, J., Haudenschild, C. C., and Zhan, X. (1998) *J. Biol. Chem.* **273,** 25770–25776
14. Schaller, M. D. (2001) *Oncogene* **20,** 6459–6472
15. Fidler, I. J., Gruys, E., Cifone, M. A., Barnes, Z., and Bucana, C. (1981) *J. Natl. Cancer Inst.* **67,** 947–956
16. Sakai, R., Iwamatsu, A., Hirano, N., Ogawa, S., Tanaka, T., Mano, H., Yazaki, Y., and Hirai, H. (1994) *EMBO J.* **13,** 3748–3756
17. Basara, M. L., McCarthy, J. B., Barnes, D. W., and Furcht, L. T. (1985) *Cancer Res.* **45,** 2487–2494
18. Hanke, J. H., Gardner, J. P., Dow, R. L., Changelian, P. S., Brissette, W. H., Weringer, E. J., Pollok, B. A., and Connelly, P. A. (1996) *J. Biol. Chem.* **271,** 695–701
19. Sakai, R., Nakamoto, T., Ozawa, K., Aizawa, S., and Hirai, H. (1997) *Oncogene* **14,** 1419–1426
20. Uruno, T., Liu, J., Zhang, P., Fan, Y., Egile, C., Li, R., Mueller, S. C., and Zhan, X. (2001) *Nat. Cell Biol.* **3,** 259–266
21. Kaksonen, M., Peng, H. B., and Rauvala, H. (2000) *J. Cell Sci.* ***113,*** 4421–4426
22. Wu, H., Reynolds, A. B., Kanner, S. B., Vines, R. R., and Parsons, J. T. (1991) *Mol. Cell. Biol.* **11,** 5113–5124
23. Cary, L. A., Chang, J. F., and Guan, J. L. (1996) *J. Cell Sci.* **109,** (suppl.) 1787–1794
24. Klinghoffer, R. A., Sachsenmaier, C., Cooper, J. A., and Soriano, P. (1999) *EMBO J.* **18,** 2459–2471
25. Zeng, L., Si, X., Yu, W. P., Le, H. T., Ng, K. P., Teng, R. M., Ryan, K., Wang, D. Z., Ponniah, S., and Pallen, C. J. (2003) *J. Cell Biol.* **160,** 137–146
26. Mariotti, A., Kedeshian, P. A., Dans, M., Curatola, A. M., Gagnoux-Palacios, L., and Giancotti, F. G. (2001) *J. Cell Biol.* **155,** 447–458
27. Wary, K. K., Mariotti, A., Zurzolo, C., and Giancotti, F. G. (1998) *Cell* **94,** 625–634
28. Schaller, M. D., Hildebrand, J. D., Shannon, J. D., Fox, J. W., Vines, R. R., and Parsons, J. T. (1994) *Mol. Cell. Biol.* **14,** 1680–1688
29. Giancotti, F. G., and Ruoslahti, E. (1999) *Science* **285,** 1028–1032
30. Schlaepfer, D. D., Broome, M. A., and Hunter, T. (1997) *Mol. Cell. Biol.* **17,** 1702–1713
31. Schlaepfer, D. D., Jones, K. C., and Hunter, T. (1998) *Mol. Cell. Biol.* **18,** 2571–2585
32. Kanner, S. B., Reynolds, A. B., Vines, R. R., and Parsons, J. T. (1990) *Proc. Natl. Acad. Sci. U. S. A.* **87,** 3328–3332
33. Zhan, X., Hu, X., Hampton, B., Burgess, W. H., Friesel, R., and Maciag, T. (1993) *J. Biol. Chem.* **268,** 24427–24431
34. Li, Y., Tondravi, M., Liu, J., Smith, E., Haudenschild, C. C., Kaczmarek, M., and Zhan, X. (2001) *Cancer Res.* **61,** 6906–6911
35. Mitchison, T. J., and Cramer, L. P. (1996) *Cell* **84,** 371–379
36. Schuuring, E. (1995) *Gene (Amst.)* **159,** 83–96
37. Patel, A. S., Schechter, G. L., Wasilenko, W. J., and Somers, K. D. (1998) *Oncogene* **16,** 3227–3232
38. Head, J. A., Jiang, D., Li, M., Zorn, L. J., Schaefer, E. M., Parsons, J. T., and Weed, S. A. (2003) *Mol. Biol. Cell* **14,** 3216–3229

The EMBO Journal (2004) 23, 1075–1088 | © 2004 European Molecular Biology Organization | All Rights Reserved 0261-4189/04
www.embojournal.org

THE EMBO JOURNAL

Tiam1 mediates neurite outgrowth induced by ephrin-B1 and EphA2

Masamitsu Tanaka[1,2], Riuko Ohashi[1,3], Ritsuko Nakamura[1], Kazuya Shinmura[1], Takaharu Kamo[1], Ryuichi Sakai[2] and Haruhiko Sugimura[1,*]

[1]First Department of Pathology, Hamamatsu University School of Medicine, Handayama, Hamamatsu, Japan and [2]Growth Factor Division, National Cancer Center Research Institute, Tsukiji, Chuo-ku, Tokyo, Japan

Bidirectional signals mediated by Eph receptor tyrosine kinases and their membrane-bound ligands, ephrins, play pivotal roles in the formation of neural networks by induction of both collapse and elongation of neurites. However, the downstream molecular modules to deliver these cues are largely unknown. We report here that the interaction of a Rac1-specific guanine nucleotide-exchanging factor, Tiam1, with ephrin-B1 and EphA2 mediates neurite outgrowth. In cells coexpressing Tiam1 and ephrin-B1, Rac1 is activated by the extracellular stimulation of clustered soluble EphB2 receptors. Similarly, soluble ephrin-A1 activates Rac1 in cells coexpressing Tiam1 and EphA2. Cortical neurons from the E14 mouse embryos and neuroblastoma cells significantly extend neurites when placed on surfaces coated with the extracellular domain of EphB2 or ephrin-A1, which were abolished by the forced expression of the dominant-negative mutant of ephrin-B1 or EphA2. Furthermore, the introduction of a dominant-negative form of Tiam1 also inhibits neurite outgrowth induced by the ephrin-B1 and EphA2 signals. These results indicate that Tiam1 is required for neurite outgrowth induced by both ephrin-B1-mediated reverse signaling and EphA2-mediated forward signaling.

The EMBO Journal (2004) **23**, 1075–1088. doi:10.1038/sj.emboj.7600128; Published online 26 February 2004
Subject Categories: signal transduction; cell & tissue architecture
Keywords: cortical neuron; Eph; ephrin; neurite outgrowth; Tiam1

Introduction

The members of the Eph receptors and their ligands are variously involved in neural development: regulating axon guidance, axon fasciculation and synaptogenesis. The interaction of Eph and ephrin regulates axon guidance by a repulsive function. Retinal axons expressing EphA receptors are guided to their target tectal area according to interactions with a repellent ephrin-A gradient (Cheng *et al*, 1995). The pathfinding of mouse anterior commissure is also regulated by the repulsive function between ephrin-B1 and EphB2 receptor (Henkemeyer *et al*, 1996). On the other hand, the interaction of Eph and ephrin also induces attractive axon guidance in certain settings. Vomeronasal axons expressing ephrin-A5 are attractively elongated by interaction with target EphA receptors in the accessory olfactory bulb, implying that ephrin-A mediates attractive guidance mechanisms (Knoll *et al*, 2001). Another example of attractive axon guidance is also reported in terms of the interaction of the EphB receptor and ephrin-B. Mann *et al* (2002) show that *Xenopus* dorsal retinal axons expressing ephrin-B preferentially project to the tectal area where EphB1 is highly expressed, while the ventral ones that express EphB2 project to the dorsal area of the tectum where ephrin-Bs are highly expressed. Therefore, Eph receptors and ephrins are involved in both repulsive and attractive guidance mechanisms during the establishment of neuronal connections. Gao *et al* have previously shown the two opposing effects of Eph receptors and ephrins on neurite outgrowth *in vitro* by a series of experiments. Primary cultured rat neurons extended or retracted neurites when they were plated on cells stably expressing various Eph or ephrins on their surface (Gao *et al*, 1996, 1998, 1999, 2000). However, the molecular basis of such morphological change requires investigation.

Rho GTPases are important regulators of the actin cytoskeleton. Activation of RhoA and its effector protein Rho-kinase (ROCK) leads to growth cone collapse, neurite retraction or neurite growth inhibition by inducing the contraction of actomyosin (Wahl *et al*, 2000). On the other hand, activation of Rac1 induces neurite elongation. Tiam1, a specific guanine-nucleotide exchange factor (GEF) for Rac1 (Habets *et al*, 1994), affects neuronal morphology (Leeuwen *et al*, 1997; Kunda *et al*, 2001). Moreover, STEF, another GEF for Rac1, which has highly homologous regions with Tiam1, is also effective in neurite outgrowth (Matsuo *et al*, 2002). The cellular localization of Tiam1 and EphA2 is similar. When cells were cultured sparsely, both EphA2 and activated Tiam1 are highly expressed at the cell periphery containing membrane ruffles. However, when cells were adhered to each other, they are highly expressed at the site of cell-to-cell adhesion (Sander *et al*, 1998; Zantek *et al*, 1999). These observations led us to focus on the examination whether Tiam1 and EphA2 interact, and Tiam1 could be a mediator of EphA2 receptor. During the examination of the interaction of Tiam1 with several Eph receptors and ephrins, we have found that ephrin-B1 also associates with Tiam1.

In this study, we describe the interaction of Tiam1 with ephrin-B1 and EphA2. A part of Tiam1 was accumulated to the sites including clustered ephrin-B1 and EphA2 after the

*Corresponding author. First Department of Pathology, Hamamatsu University School of Medicine, 1-20-1 Handayama, Hamamatsu 431-3192, Japan. Tel.: +81 53 435 2220; Fax: +81 53 435 2225; E-mail: hsugimur@hama-med.ac.jp
[3]Present address: Division of Cellular and Molecular Pathology, Department of Cellular Function, Niigata University Graduate School of Medical and Dental Sciences, Asahimachi-dori 1, Niigata 951-8510, Japan

Received: 9 April 2003; accepted: 19 January 2004; published online: 26 February 2004

cells were stimulated with EphB2 and ephrin-A1, respectively. Neurite outgrowth was observed in primary cortical neurons from mouse embryos in response to the stimulation of EphB2-Fc, and NB1 neuroblastoma cells in response to ephrin-a1-Fc. Coexpression of the dominant-negative mutant of Tiam1, or mutant of ephrin-B1 or EphA2, which lacks its cytoplasmic region prevented the neurite extension described above. These results suggest that Tiam1 is a mediator of ephrin-B1- and EphA2-induced neurite outgrowth.

Results

Tiam1 interacts with the cytoplasmic domain of ephrin-B1 and EphA2

We have examined the association between Tiam1 with ephrin-B1 and EphA2 *in vivo*. Coexpression and co-precipitation analysis in COS1 cells revealed that Tiam1 was co-precipitated with ephrin-B1 and EphA2 by specific antibodies (Figure 1A, lanes 1 and 3, arrowheads, respectively), but not by the normal goat serum or mouse IgG1 (Figure 1A, lanes 2 and 4, arrowheads, respectively). These results were further confirmed by experiments using the antibodies in reverse order. Ephrin-B1 and EphA2 were co-precipitated with Tiam1 (Figure 1A, lanes 5 and 7, arrowheads, respectively). Next, we have generated several truncated mutants of Tiam1 to determine the region within Tiam1, which is required for the interaction with ephrin-B1 or EphA2 (Figure 1B). Among the truncated mutants of Tiam1, N-terminal-deleted Tiam1 (C1199) tightly bound to ephrin-B1, but Tiam1 encoding 392 amino-terminal amino acids (N392) did not associate with ephrin-B1 (Figure 1C, lanes 1–4). Reciprocally, EphA2 interacted with Tiam1 (N392), but did not associate with Tiam1 (C1199) (Figure 1C, lanes 5–8). These results indicate that ephrin-B1 and EphA2 interact with different regions of Tiam1.

To identify the region of the Tiam1 protein essential for the interaction with ephrin-B1 or EphA2, we performed an *in vitro* glutathione *S*-transferase (GST) fusion protein pull-down assay. *In vitro*-translated Tiam1 was co-precipitated with the GST-tagged cytoplasmic region of ephrin-B1 (ephrin-B1$^{264-346}$) or EphA2 (EphA2$^{563-977}$) but not by the control GST alone (Figure 2, top). The cytoplasmic region of ephrin-B1 did not bind to Tiam1 (N392). As shown in Figure 2 (bottom), ephrin-B1 clearly associated with the PHnTSS region of Tiam1, which is also included in C1199 and N1041. Therefore, we concluded that the cytoplasmic region of ephrin-B1 binds to Tiam1 via its PHnTSS region. The PHnTSS region contains amino-terminal PH domain, which is known to involve in membrane targeting of Tiam1 protein, and TSS domain, which is conserved among Tiam1, STEF and SIF proteins (Matsuo *et al*, 2002). On the other hand, the GST-tagged cytoplasmic region of EphA2 did not associate with the PHnTSS region of Tiam1, but instead associated with Tiam1 constructs harboring the amino-terminal region of Tiam1 (N392). We assume that EphA2 binds to Tiam1 via its amino-terminal region (Tiam1$^{1-392}$). Although the association of Tiam1 with ephrin-B1 was detected without activation of ephrin-B1 by the extracellular domain (ECD) of EphB2, we found that the GST-tagged PHnTSS domain of Tiam1 expressed in 293T cells was co-precipitated with ephrin-B1 more effectively after the incubation with EphB2-Fc (Supplementary information 3A).

Finally, we examined the *in vivo* status of Tiam1 with ephrin-B1/EphA2 in the E14 mouse brain, where Tiam1 and ephrin-B1 are highly expressed. Tiam1 was co-precipitated with ephrin-B1 from an extract of E14 mouse whole brain by the specific antibody, but not by normal goat serum (Figure 3A). Although EphA2 in the whole brain of E14 mouse is expressed at a low level, endogenously expressed Tiam1 protein was co-immunoprecipitated with EphA2 but not with the control mouse IgG1 (Figure 3B). The interaction of ephrin-B1 and EphA2 with Tiam1 in the mouse brain was further confirmed by experiments using the antibodies in reverse order. Ephrin-B1 and EphA2 were co-precipitated with Tiam1 by the specific antibodies, but not by normal rabbit serum (Figure 3C and D). The size of endogenous ephrin-B1 protein in the mouse brain was slightly larger than transiently expressed ephrin-B1 in COS1 cells.

Tiam1 is translocated after stimulation with the extracellular domain of EphB2 or ephrin-A1

Next, we examined the cellular localization of Tiam1, ephrin-B1 and EphA2. Ephrin-B reverse signaling is known to induce the formation of large membrane patches containing several proteins after stimulation with preclustered EphB2-Fc (Cowan and Henkemeyer, 2002; Palmer *et al*, 2002). In SK-N-MC cells, intense staining of endogenous ephrin-B1 protein is observed in the cell membrane at the contact of cell-to-cell adhesion (Figure 4A, column c, top). Concomitantly with the stimulation of EphB2-Fc, patches containing ephrin-B1 were formed mostly in the cell membrane (Figure 4A, column a, top panel). As expected, the colocalization of ephrin-B1 in patches containing EphB2-Fc was also confirmed in SK-N-MC cells (Supplementary information 2, column a). Tiam1 protein is homogenously expressed in the cytoplasm before

Figure 1 Tiam1 forms a complex with ephrin-B1 and EphA2 receptor. (**A**) COS1 cells were transiently transfected with a plasmid encoding wild-type Tiam1 together with that encoding ephrin-B1 (lanes 1, 2, 5, 6) or EphA2 (lanes 3, 4, 7, 8). Cells were lysed and immunoprecipitated (IP) with anti-ephrin-B1 (goat polyclonal, lane 1), normal goat serum (NGS, lane 2), anti-EphA2 (lane 3), mouse IgG1 (lane 4), anti-Tiam1 (lanes 5, 7) or normal rabbit serum (NRS, lanes 6, 8). The precipitates were subjected to immunoblotting (IB) with the indicated antibodies. The same membranes were reblotted with the antibodies indicated (bottom panels). The expression of Tiam1, ephrin-B1 and EphA2 in the cell lysate was confirmed by immunoblotting. When wild-type ephrin-B1 is overexpressed in COS1 cells, at least two major bands were observed by anti-ephrin-B1 goat polyclonal antibody. Ig, immunoglobulin. The prominent band of 80 kDa in lane 3 is an unknown protein, which associates with EphA2 and may have a related structure with Tiam1. (**B**) Schematic representation of a wild-type and the truncated Tiam1 cDNA constructs used in this study. Proteins are depicted to scale; M, myristoylation signal; PHn and PHc, NH2- and COOH-terminal pleckstrin homology domains; TSS, otherwise known as coiled-coil region and an additional adjacent region (CC-Ex); PDZ, PSD-95/DlgA/ZO-1 domain; DH, Dbl homology domain. (**C**) COS1 cells were transiently transfected with the plasmids as indicated in the above lanes. The cell lysates were immunoprecipitated with anti-ephrin-B1 C18 (lanes 1, 3), EphA2 (lanes 5, 7), normal rabbit serum (lanes 2, 4) or mouse IgG1 (lanes 6, 8) and immunoblotted with anti-myc antibody. The same membranes were reblotted with anti-ephrin-B1 (goat) or anti-EphA2 as indicated. The expression of myc-tagged Tiam1 constructs in these cell lysates (total lysate) was confirmed by immunoblotting. The additional band at 110 kDa in lane 1 may be an artificially produced fragment of overexpressed Tiam1 construct.

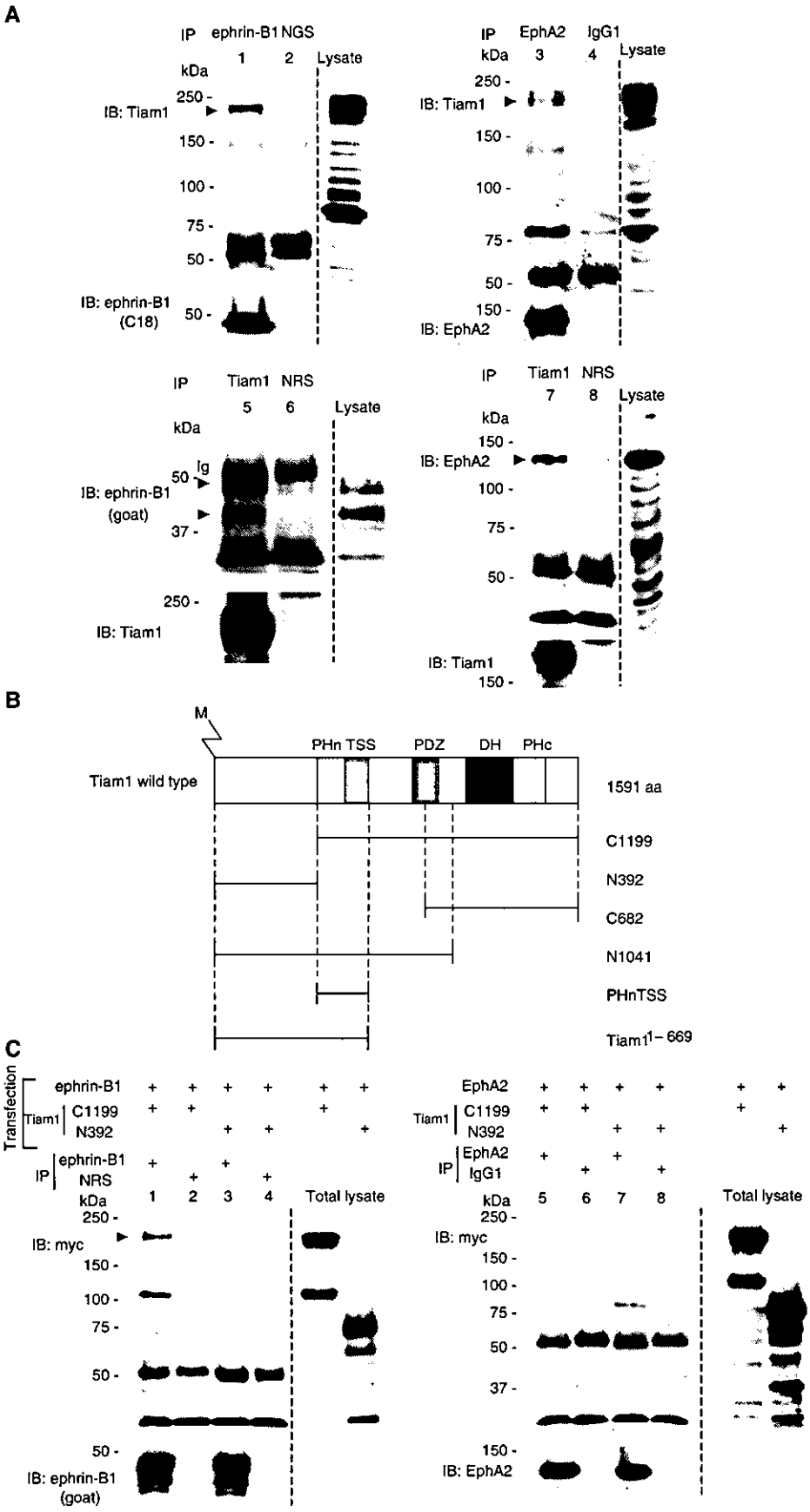

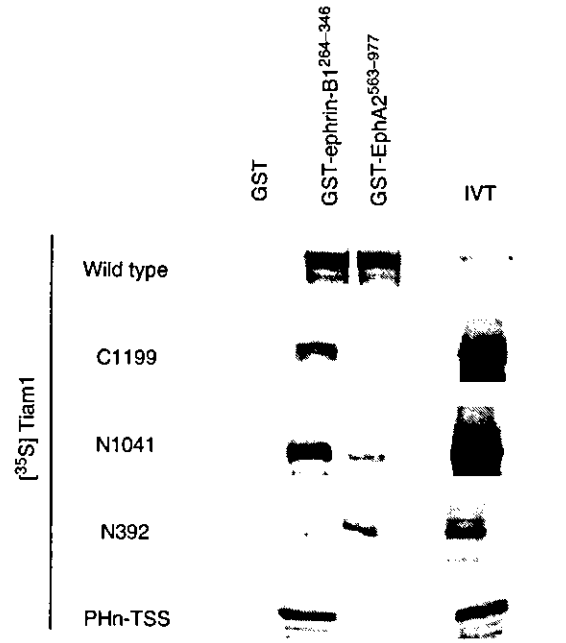

Figure 2 Tiam1 binds to ephrin-B1 and EphA2 *in vitro*: [^{35}S]methionine -labeled wild type or truncated mutants of Tiam1 (C1199, N1041, N392, PHnTSS) translated products were incubated with glutathione–agarose-conjugated GST, GST-ephrin-B1$^{264-346}$ and GST-EphA2$^{563-977}$, respectively. IVT, the input of *in vitro* translation reaction before the beads binding.

stimulation with EphB2-Fc (Figure 4A, column c, middle). However, at least a part of Tiam1 was clearly found to colocalize to the patches after exposure to preclustered EphB2-Fc (Figure 4A, column a, middle and bottom). Although there were a few spotty stains of both ephrin-B1 and Tiam1 in the cells without stimulation of EphB2-Fc, they never colocalized as shown in the merged panel (Figure 4A, column c). In order to exclude the possibility that the second antibodies used directly recognize the clustered Fc fusion proteins, we have shown that there is almost no staining of Tiam1 protein by staining with the secondary antibody without prior incubation with the primary anti-Tiam1 antibody (Figure 4A, column b). We also confirmed that the preincubation of anti-Tiam1 antibody with the blocking peptide (Tiam1 C16) or the bacterially produced GST fusion protein of Tiam1$^{1430-1591}$ containing its C-terminal region abolished Tiam1 staining (data not shown). In the primary cortical neurons from E14 mouse embryos, ephrin-B1 is highly expressed on the cell membrane and neurites, and Tiam1 protein is distributed in the cytoplasm of the cell body and neurites (Figure 4B, columns c and d). Tiam1 and ephrin-B1 were also copatched in E14 cortical neurons 1 h after stimulation with clustered EphB2-Fc (Figure 4B, columns a and b). We observe many patches containing Tiam1 and ephrin-B1 on the elongated neurites and the periphery of cell bodies of these neurons, while there was no such patchy localization of Tiam1 in the neurons without stimulation with EphB2-Fc. In Supplementary information 2, we show the precise colocalization of ephrin-B1 with EphB2-Fc patches, and that in the control there was no crossreaction of the rhodamine-labeled secondary antibody to clustered Fc fusion protein in primary cortical neurons (columns b and c, respectively).

NB1 neuroblastoma cells express EphA2 and Tiam1 endogenously as described later. Before stimulation of NB1 cells with ephrin-A1-Fc, there was no patchy localization of EphA2 detected by immunostaining. Intense staining of EphA2 was located on the cell membrane, especially at the sites of cell-to-cell contact (Figure 4C, column c, top). In the same manner as is the case with cortical neurons, Tiam1, initially distributed homogenously in the cytoplasm (Figure 4C, column c, middle), was partly translocated to patches containing EphA2 after stimulation with soluble ephrin-A1 (Figure 4C, column a, middle and bottom). The patches containing EphA2 localized not only on the cell membrane but also in the cytoplasm, which may be a consequence of the internalization of EphA2 from the cell membrane after stimulation of its ligand. Such internalization of ligand-stimulated EphA2, and more recently ephrin-B1, has been reported (Walker-Daniels *et al*., 2002; Zimmer *et al*., 2003). There was no crossreaction of the secondary antibody to the clustered ephrin-A1-Fc protein (Figure 4C, column b). These results together demonstrate the colocalization of Tiam1 with ephrin-B1 and EphA2, and the distribution of Tiam1 is at least partly translocated after stimulation of ephrin-B1 and EphA2.

Tiam1 is involved in Rac1 activation induced by Eph/ephrin signaling

To analyze whether Eph/ephrin signaling mediates Tiam1 activation, we examined the modification of Tiam1-induced Rac1 activation by the affinity precipitation of GTP-bound Rac1 with the GST-tagged p21-binding domain of PAK1 (GST-PBD). Rac1 was slightly activated by the overexpression of wild-type Tiam1 (Figure 5A, compare lanes 1 and 2). Although Rac1 was also slightly activated after stimulation with EphB2-Fc in ephrin-B1-expressing cells (Figure 5A, lane 3), the amount of GTP-bound Rac1 was markedly increased in response to the stimulation by EphB2-Fc when both Tiam1 and ephrin-B1 are expressed (Figure 5A, compare lanes 4 and 5). Because the PHnTSS region of Tiam1 works as a dominant-negative mutant of Tiam1 (Stam *et al*, 1997), we next examined whether PHnTSS of Tiam1 blocks the Rac1 activity induced by the activation of ephrin-B1. The activation of Rac1 induced by the stimulation of EphB2-Fc was completely abolished by the coexpression of PHnTSS of Tiam1, but not by the coexpression of Tiam1 (N392) (Figure 5A, lanes 8 and 9). The coexpression of EphA2 and Tiam1 did not induce Rac1 activation significantly without stimulation of ephrin-A1-Fc (Figure 5A, lane 10). The overexpression of EphA2 alone is not effective in activating Rac1 even though the cells were stimulated by ephrin-A1 (Figure 5A, lane 15). The stimulation of ephrin-A1-Fc activated Rac1 in cells expressing EphA2 and Tiam1, which was blocked by the coexpression of Tiam1$^{1-669}$ (Figure 5A, compare lanes 11 and 12). The coexpression of PHnTSS partly inhibited the ephrin-A1-Fc-induced Rac1 activation, and Tiam1$^{1-392}$ blocked the Rac1 activation very effectively but not completely (Figure 5A, lanes 13 and 14).

We next examined the phosphorylation of Tiam1 by the activation of ephrin-B1 or EphA2. When ephrin-B1-expressing cells were cocultured with cells expressing kinase-inactivated EphB2 (EphB2K661M), ephrin-B1 was highly phosphorylated on tyrosine residues, but not when cocultured with control mock-transfected cells as we have described before (Figure 5B, lanes 1 and 2, bottom) (Tanaka *et al*, 2003). Similarly, the tyrosine phosphorylation of EphA2 was in-

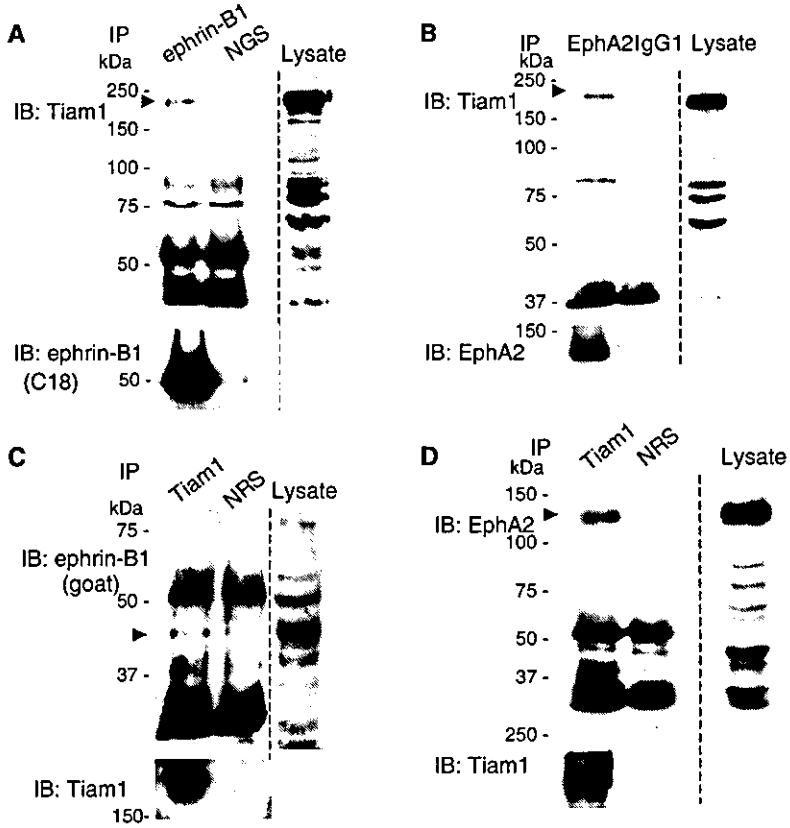

Figure 3 Tiam1 physiologically interacts with ephrin-B1 and EphA2 in the brain of an E14 mouse embryo. Whole brains from E14 mice embryos were lysed and immunoprecipitated (IP) with anti-ephrin-B1 (goat), anti-EphA2, anti-Tiam1, normal goat serum (NGS), normal rabbit serum (NRS) or mouse IgG1 respectively as indicated in the above lanes. The precipitates were subjected to immunoblotting (IB) with the indicated antibodies. Co-precipitated Tiam1, ephrin-B1 and EphA2 are indicated by arrowheads. In (C), the upper band of ephrin-B1 was overlapped with the band of immunoglobulin. The membranes were reblotted with antibodies indicated (bottom panels).

creased when EphA2-expressing cells were cocultured with cells expressing ephrin-A1 (Figure 5B, lanes 5 and 6, bottom). The activation of ephrin-B1 by overlaying the EphB2-expressing cells leads to weak phosphorylation of Tiam1 as detected by labeling cells with orthophosphate (Figure 5B, lanes 1 and 2). Tiam1 is also phosphorylated upon stimulation of EphA2 by coculturing with cells expressing ephrin-A1 (Figure 5B, lanes 3 and 4). Moreover, Tiam1 is phosphorylated on tyrosine residues by the stimulation of EphA2-mediated signaling, as detected by immunoblotting with anti-phosphotyrosine antibody (Figure 5B, lanes 5 and 6). On the other hand, we did not clearly detect phosphorylation of Tiam1 in response to activation of ephrin-B1 on either tyrosine residues (examined by the same method as above) or on serine/threonine residues by immunoblotting with the antibodies described in Supplementary information 1 (data not shown).

Neurite outgrowth by ephrin-B1–Tiam1 and EphA2–Tiam1 interaction

We first confirmed that the dissociated primary cultured cells of E14 cortical neurons still maintain the expression of Tiam1, ephrin-B1, EphB2 and EphA4 *in vitro*, although the expression levels of these proteins were higher in the cortical tissue compared to dissociated cortical cells (Figure 6E). When E14 cortical neurons were seeded on preclustered EphB2-Fc-coated plates, ephrin-B1 is phosphorylated on tyrosine residues at 30 min and 4 h after plating (Figure 6E, bottom). Around 31% of the cells seeded on EphB2-Fc-coated plates show neurites longer than one cell body in length (Figure 6A, Table I), which is statistically different from the numbers when plated on the clustered Fc only or on the albumin (Figure 6B and C). The effect of ephrin-A1-Fc on neurite outgrowth of E14 mouse cortical neurons was weaker than the stimulation of EphB2-Fc (Figure 6D, Table I). In particular, the number of cells bearing longer neurites (longer than three cell bodies in length) was much smaller when cells were seeded on ephrin-A1-Fc-coated plates than on EphB2-Fc-coated plates (Table I). EphA2 expression in the cortex of E14-16 was monitored in brain lysates, because we suspect that the weak expression in this area and the developmental stage may be one of the reasons for the less dramatic effect on neurite outgrowth. Actually, the expression of EphA2 was barely detectable in the cortex region of this stage (Figure 6E), while it was detectable in the whole brain lysate (Figure 3). We did not observe any elongated neurites on ephrin-B1-Fc-coated plates (data not shown).

In the neuroblastoma cell line NB1, a considerable expression of Tiam1 and EphA2 was detected (Figure 7D). We also confirmed that NB1 cells do not express detectable level of EphA4 (Figure 7D). We used this NB1 system in the following experiments for evaluation of EphA2 forward signaling. The

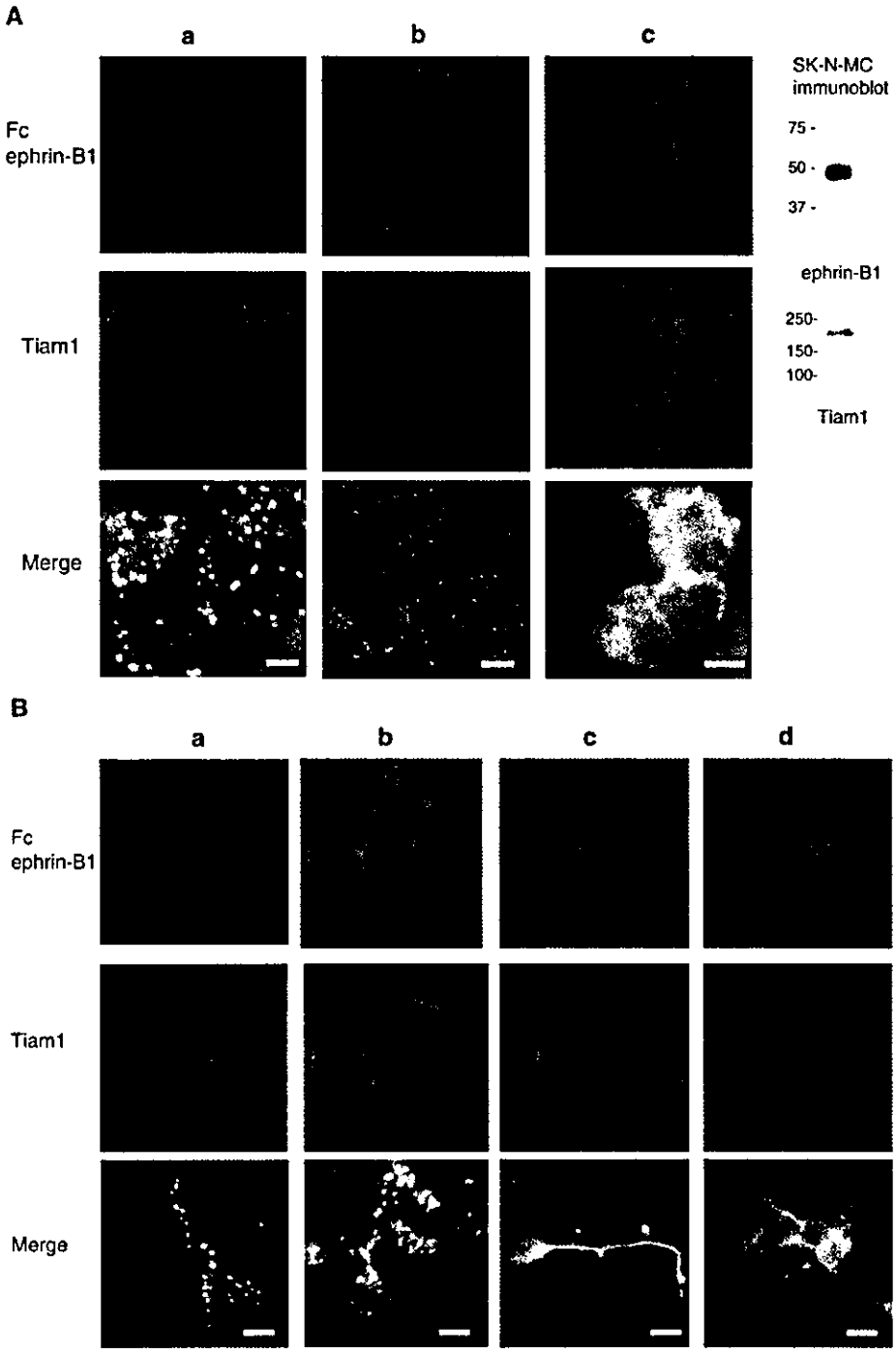

Figure 4 Tiam1 is recruited to patches induced by EphB2-Fc- or ephrin-A1-Fc stimulation. (**A**) SK-N-MC cells expressing ephrin-B1 were stimulated with 4 μg/ml of clustered EphB2-Fc (columns a, b) or left untreated (column c). After 10 min of stimulation, the cells were washed and incubated in a medium without EphB2-Fc for 1 h prior to fixation. The cells were immunostained with anti-Fc (green) and anti-Tiam1 (red) antibodies (column a). In column b, incubation with primary anti-Tiam1 antibody was omitted prior to incubation with the rhodamine-labeled secondary antibody. Column c shows the signals with anti-ephrin-B1 staining (green) and anti-Tiam1 staining (red). Expressions of Tiam1 and ephrin-B1 in SK-N-MC cells are shown by immunoblot. (**B**) (Columns a, b) E14 mouse cortical neurons were cultured for 20 h on poly-L-lysine-coated slides, and then stimulated with EphB2-Fc for 1 h as described above. The cells were fixed and immunostained with anti-Fc (green) and anti-Tiam1 (red) antibodies. (Columns c, d) Localization of ephrin-B1 (green) and Tiam1 protein (red) without stimulation of EphB2-Fc is shown. (**C**) (Columns a, b) NB1 neuroblastoma cells were stimulated with 4 μg/ml of clustered ephrin-A1-Fc as described in (A). The cells were immunostained with anti-Fc (green) and anti-Tiam1 (red) antibodies. In column b, incubation with primary anti-Tiam1 antibody was omitted prior to incubation with the rhodamine-labeled secondary antibody. (Column c) Localization of EphA2 (green) or Tiam1 protein (red) without stimulation of ephrin-A1-Fc is shown. Scale bar, 10 μm.

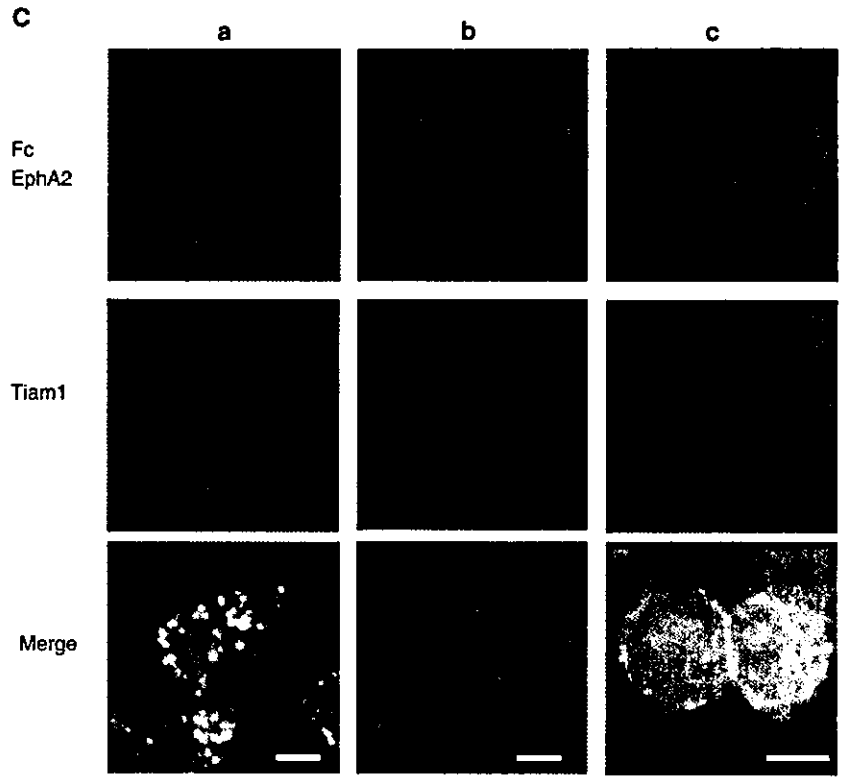

Figure 4 (Continued)

tyrosine phosphorylation of EphA2 was clearly demonstrated at 30 min and 4 h after plating on ephrin-A1-Fc-coated dish (Figure 7D, bottom). The decreased expression level of EphA2 after stimulation is considered to be a result of negative regulation of activated EphA2 by Cbl-mediated ubiquitination (Wang *et al*, 2002). When NB1 cells were plated on a surface coated with preclustered ephrin-A1-Fc, many cells exhibited long thin neurites after 16 h of incubation (Figure 7B), whereas few cells bearing such neurites were observed in cells plated on the control Fc-coated plates (Figure 7A). The elongated neurites were not observed on preclustered EphA2-Fc-coated plate, either, as shown in Figure 7C.

To confirm that the outgrowth of neurites observed above depends on the interaction of EphB2 or ephrin-A1 with its cognate ligand or receptor, we did several experiments interfering with this pathway by a soluble ligand or receptor and a dominant-negative or defective competitor in the following experiments. When the cells were plated on Fc fusion protein-coated surface as above with an excess volume of the soluble ephrin-B1-Fc or EphA2-Fc in the medium, the neurite outgrowth of E14 cortical neurons plated on the EphB2-Fc surface and neurite outgrowth of NB1 cells plated on the ephrin-A1-Fc surface were blocked, respectively. However, the addition of soluble ephrin-B1 or EphA2 in the medium had no effect on the nonspecific neurite outgrowth of E14 cortical neurons and NB1 cells induced by plating cells on a poly-L-lysine-coated surface (data not shown). Furthermore, the forced expression of an ephrin-B1 mutant lacking its cytoplasmic region (ephrin-B1$^{1-265}$) in E14 mouse cortical neurons lessened the effect both in numbers and length of neurites, while the expression of control EGFP did not affect the neurite outgrowth (Figure 8, compare A and B). Likewise, the expression of mutants of EphA2 lacking its cytoplasmic region (EphA2$^{1-540}$) in neuroblastoma cells reduced the number of these cells bearing neurites on an ephrin-A1-coated surface (Figure 8, compare E and F).

Finally, we examined whether dominant-negative mutants of Tiam1 inhibit the neurite outgrowth induced by the ephrin-B1- or EphA2-mediated signaling. E14 cortical neurons on the EphB2-Fc surface were transiently transfected with the PHnTSS region of Tiam1 tagged with EGFP. On the other hand, we used Tiam1$^{1-669}$ to test whether it could block the neurite outgrowth induced by EphA2-mediated signaling, because it effectively blocked the Rac1 activation induced by the activation of EphA2 (Figure 5A). As shown in Figure 8C, the neurite outgrowth of cortical neurons on the EphB2-Fc surface was significantly inhibited by the expression of PHnTSS protein. Similarly, NB1 cells expressing Tiam1$^{1-669}$ did not show apparent neurites on the ephrin-A1-Fc-coated surface (Figure 8G). On the other hand, the expression of these Tiam1 fragments did not effectively inhibit the nonspecific neurite outgrowth of cortical neurons and NB1 cells induced by plating the cells on poly-L-lysine-coated plates (data not shown). Moreover, the inhibitory effect of PHnTSS protein on the neurite outgrowth of NB1 cells on the ephrin-A1-Fc-coated surface was modest, and we did not observe any inhibition of neurite outgrowth by Tiam1$^{1-392}$ in cortical neurons on the EphB2-Fc-coated surface (data not shown). Taken together, these results (Figure 8D and H)

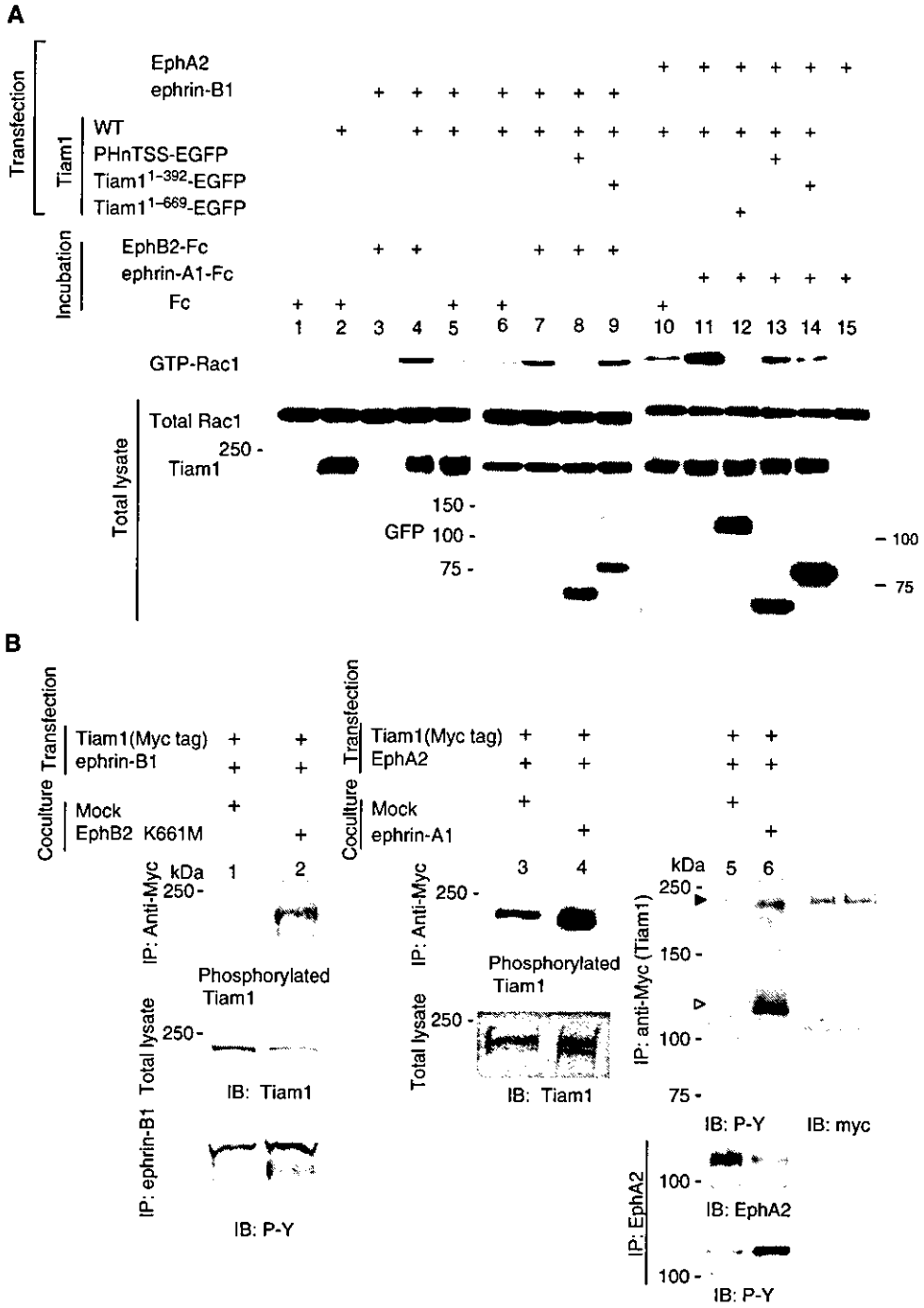

Figure 5 Tiam1 mediates Eph/ephrin-mediated signaling cascades leading to Rac1 activation. **(A)** COS1 cells were transiently transfected with 2 μg of a plasmid encoding wild-type Rac1, together with plasmids indicated in the above lanes. Mock plasmid was used to adjust the amount of DNA to total 10 μg for each transfection. The transfected cells were incubated in media containing clustered EphB2-Fc, ephrin-A1-Fc or control Fc each at a concentration of 5 μg/ml as indicated above the lanes for 15 min before harvesting the cell lysates for affinity precipitation with immobilized GST-PBD. Precipitated GTP-bound Rac1 was detected by immunoblotting with anti-Rac1 antibody. Expression of total Rac1 and Tiam1 is shown at the bottom. **(B)** Phosphorylation of Tiam1 induced by the activation of ephrin-B1 or EphA2 *in vivo*. 293T cells transfected with the plasmids indicated at the top were cocultured with the 293T cells (lane 1), the 293T cells stably expressing EphB2 K661M (lane 2), the NIH3T3 cells (lanes 3, 5) or the NIH3T3 cells stably expressing ephrin-A1 (lanes 4, 6). Lanes 1–4: The coculture was performed in media containing $^{32}P_i$ for 4 h, and then the cells were lysed for immunoprecipitation with anti-myc, separated by SDS–PAGE and visualized by autoradiography. Lanes 1, 2 bottom: The lysates for immunoprecipitation were prepared from the cells as described above except for the labeling with $^{32}P_i$. Lanes 5, 6: The coculture was performed for 30 min before cell lysates were immunoprecipitated with anti-myc and immunoblotted with anti-phospho-tyrosine antibody (4G10). The phosphorylation of Tiam1 is indicated by filled triangle. Co-precipitated EphA2 is indicated by open triangle. The same membrane was reblotted with anti-myc antibody (right panel). The phosphorylation of ephrin-B1 and EphA2 on tyrosine residues is shown at the bottom of lanes 1, 2 and lanes 5, 6, respectively.

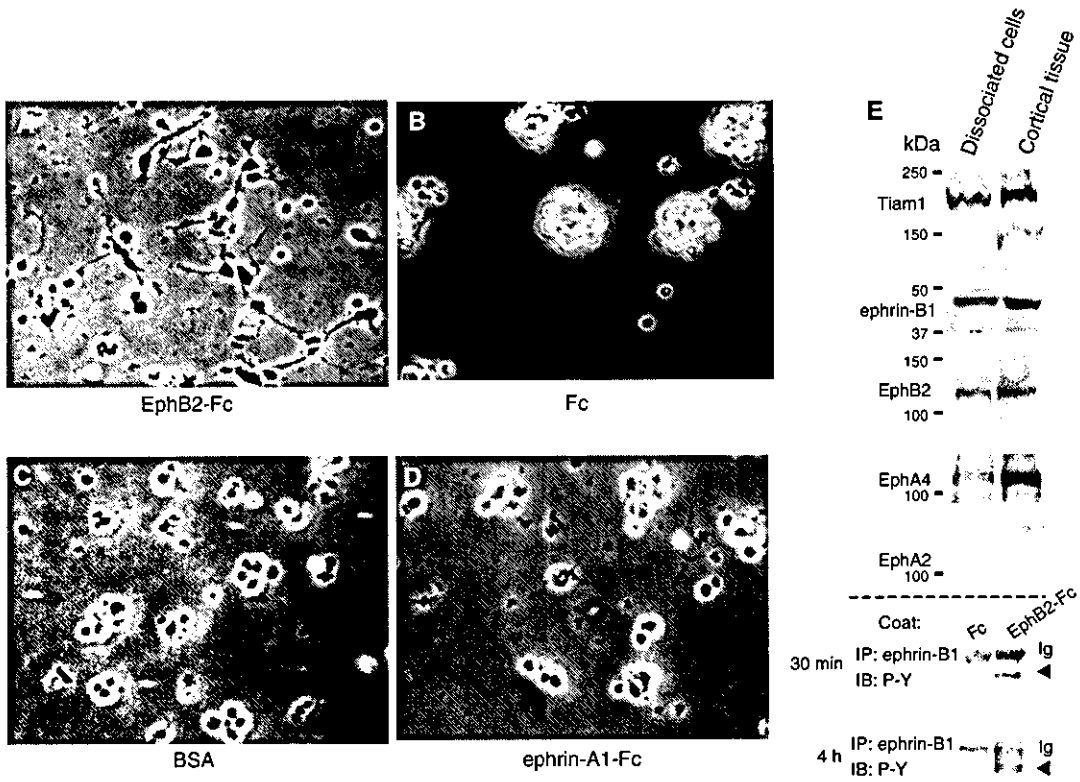

Figure 6 EphB2-Fc induces neurite outgrowth of E14 mouse cortical neurons. Primary cultured cortical neurons from E14 mouse cerebral cortex were seeded on plates coated with EphB2-Fc (**A**), Fc fragment (**B**), bovine serum albumin (BSA) (**C**) or ephrin-A1-Fc (**D**), as described in Materials and methods (Neurite elongation assay). Representative pictures are shown after incubation for 20 h (A–D). (**E**) Expression of Tiam1, ephrin-B1 and various Eph receptors in dissociated primary cultured cells after 20 h incubation on poly-L-lysine-coated dishes, or in the cortical tissues was monitored by immunoblotting. (E, bottom) E14 primary precursors plated on an EphB2-Fc-coated dish were lysed for the indicated period, and immunoprecipitated with anti-ephrin-B1. Tyrosine phosphorylation of ephrin-B1 is shown by immunoblotting.

Table I Quantification of the effects of EphB2-Fc and ephrin-A1-Fc on neurite formation

	Three cell bodies/ total counted[a]	One cell body/total counted[a]
E14 primary cortical neuron[b]		
Fc	0/527 (0%)	0/527 (0%)
BSA	0/531 (0%)	31/531 (5.8%)
EphB2-Fc	61/552 (11.1%)	173/552 (31.3%)
ephrin-A1-Fc	10/523 (1.95)	99/523 (18.9%)
NB1 neuroblastoma cell line[c]		
Fc		0/323 (0%)
ephrin-A1-Fc		115/349 (33.0%)
EphA2-Fc		14/304 (4.6%)

[a]The number of cells possessing neuritis three cell bodies or one cell body was counted 20 h after plating the cells.
[b]Total number of cells counted in four independent experiments.
[c]Total number of cells counted in three independent experiments.

indicate that Tiam1 locates downstream of ephrin-B1- or EphA2-mediated signaling and is involved in the neurite outgrowth.

Discussion

Examination of the association between Tiam1 with ephrin-B1 and EphA2 receptor revealed that Tiam1 interacts with ephrin-B1 and EphA2. Interaction of Tiam1 with EphA2 was not apparently modified by the phosphorylation status of EphA2, because EphA2 with a mutation in its kinase domain and an abolished catalytic activity also associated with Tiam1 as well as wild-type EphA2 (data not shown). However, we cannot completely exclude the possibility that the association of Tiam1 with ephrin-B1 is increased by the stimulation of EphB2-Fc (Supplementary information 3A). The observations that staining of Tiam1 in the cytoplasm did not appear to diminish in the stimulated cells (Figure 4) reveal that only a part of Tiam1 protein translocated to the patches colocalizing with ephrin-B1 or EphA2. Therefore, the localized activation of Tiam1 and Rac1 should be monitored spatially and temporally in these cells in order to evaluate the significance of the translocation of Tiam1. In primary cultured cortical neurons, patches containing ephrin-B1 and Tiam1 often locate along the extended neurites. The biological significance of such colocalization along the neurites requires elucidation. Although Tiam1 is clearly phosphorylated on tyrosine residues by EphA2 activation, we detected phosphorylation of Tiam1 in ephrin-B1-activated cells at low level only by the orthophosphate labeling (Figure 5B). Because the phosphorylation of Tiam1 on threonine residues has been detected by the same antibody in response to the stimulation of platelet-derived growth factor, Tiam1 was not phosphorylated at least on the same positions by the activation of ephrin-B1 (Fleming *et al*, 1998). The significance of the

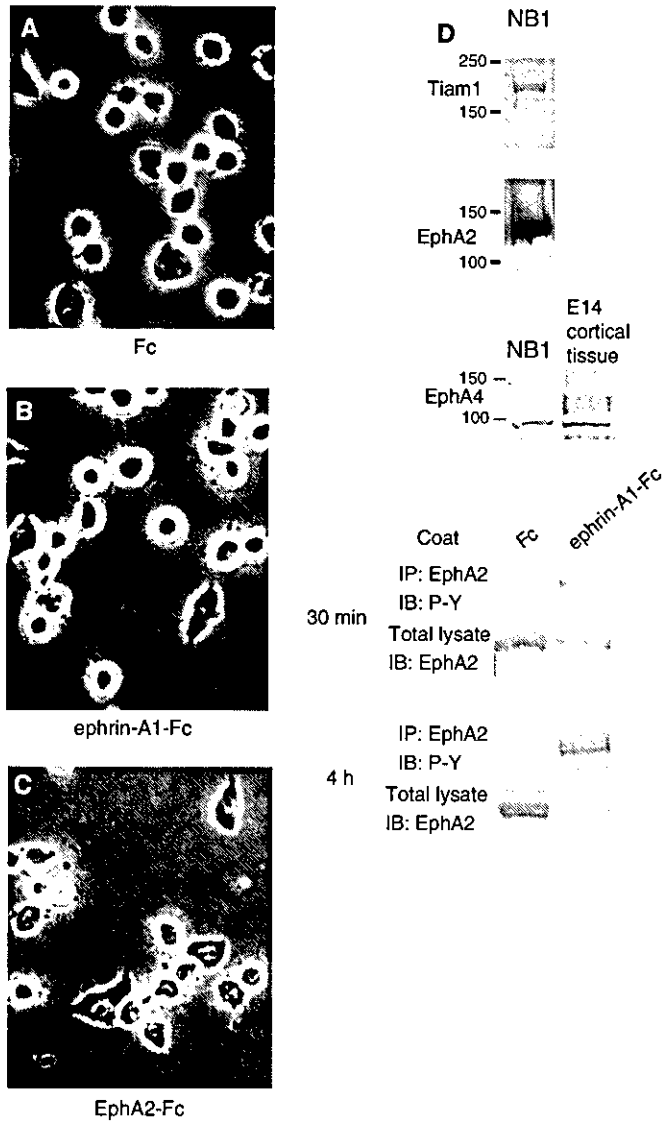

Figure 7 Ephrin-A1-Fc induces neurite outgrowth of NB1 neuroblastoma cells. NB1 neuroblastoma cells were seeded on plates coated with Fc fragment (**A**), ephrin-A1-Fc (**B**) or EphA2-Fc (**C**) as described in Materials and methods. Representative cells are shown after incubation for 20 h (A–C). (**D**) Expression of Tiam1 and Eph receptors in NB1 cells is shown by immunoblotting. (D, bottom) The NB1 cells plated on ephrin-A1-Fc-coated dishes were lysed for the indicated period, and immunoprecipitated with anti-EphA2. Tyrosine phosphorylation of EphA2 is shown by immunoblotting.

phosphorylation of Tiam1 induced by the activation of ephrin-B1 and EphA2 remains to be further studied.

Among proteins reported to be putatively associated with the cytoplasmic regions of Ephs or ephrins, Ephexin, which is a GEF for the rho family GTPases, preferentially interacts with EphA receptors (Shamah *et al*, 2001). Stimulation of ephrin-A regulates growth cone collapse or retraction through Ephexin. Although A-class ephrins are not highly expressed in the developing mouse cortex (Yun *et al*, 2003), it is important to examine the expression of Tiam1 and Ephexin, two exchange factors having opposing effects on the neurites motility, in the cortical region. Furthermore, we also have to consider a homologous protein of Tiam1, STEF, another GEF for Rac1, because STEF is also expressed in the cerebral cortex of developing mice (Matsuo *et al*, 2002; Kawauchi *et al*, 2003). We detected the association of the PHnTSS domain

Figure 8 Expression of dominant-negative mutants of ephrin-B1, EphA2 and Tiam1 affects EphB2-Fc- or ephrin-A1-Fc-induced neurite outgrowth. Primary cultured cortical neurons from E14 mouse embryos (**A–D**), or NB1 cells (**E–H**) were transfected with plasmids encoding either EGFP, EGFP-tagged mutants of ephrin-B1 or EphA2, which lack the cytoplasmic regions (ephrin-B1$^{1-265}$-EGFP, EphA2$^{1-563}$-EGFP), or EGFP-tagged fragments of Tiam1 (PHnTSS-EGFP or Tiam1$^{1-669}$-EGFP). The transfected cells were fixed after 20 h of incubation on slides coated with either EphB2-Fc (A–D) or ephrin-A1-Fc (E–H), and observed through a fluorescence microscope. Representative cells are shown (A–C, E–G). (D, H) Percentage of transfected cells bearing neurites longer than one cell body. Exogenously expressed proteins in these cells were monitored by immunoblotting.